Purification of a subset of *Saccharomyces cerevisiae* peroxisomal proteins

by

Tuhin Kumar Guha

A thesis submitted to the Faculty of Graduate Studies of

The University of Manitoba

in partial fulfillment of the requirements for the degree of

MASTER OF SCIENCE

Department of Microbiology

University of Manitoba

Winnipeg, Manitoba

Canada

ABSTRACT

Peroxisomes are ubiquitous and are considered to be vital organelles in eukaryotic cells; however, unlike mitochondria and chloroplast, they lack DNA and a protein secretory apparatus. Therefore, peroxisome biogenesis requires a group of proteins called peroxins encoded by the *pex* genes. Out of the thirty two known peroxins discovered so far, a subset of peroxins including enzyme IDP3 and proteins namely, PEX18, PEX21 and PEX6 were chosen for this research. IDP3 plays a vital role in peroxisomal metabolism where it generates NADPH which in turn is needed by the peroxisomal enzymes to degrade unsaturated fatty acids. PEX18 and PEX21 are mutually redundant but essential for the transport of PTS2 targeted proteins into the peroxisome. PEX6 is involved in the ATP-dependent recycling of the protein receptor from the peroxisomal membrane to the cytosol. Expression plasmids were constructed that encoded each of these proteins in tandem with a histidine tag at either or both the amino and carboxy terminals of the protein. The purification of IDP3 was achieved using affinity chromatography on a nickel resin. After several unsuccessful attempts using ion exchange and size exclusion chromatography, PEX18 and PEX21 were purified by nickel affinity chromatography after denaturation to expose their His tags. The expression of PEX6 was poor by comparison with the other proteins and the low amount of protein precluded a complete purification. Future work will involve crystal screen trials, X-ray diffraction and structure refinement.

ACKNOWLEDGEMENTS

First and foremost, I would like to thank my supervisor Dr. Peter C Loewen for giving me the opportunity to work in his lab and for the immense guidance and continuous support over the past two and half years. His patience and devotion to his research will be an inspiration for me throughout my future career. I would like to thank my lab members, Mr. Jack Switala, Mrs. Jacylyn Villanueva, Dr. Ben Wiseman, Dr. Vikash Jha, Ms. Munmun Santi Nandi, Mr. Jason Chan for all their suggestions, technical help and above all for being good friends of mine. I would like to extend my gratitude and thanks to my committee members, Dr. Brian Mark, Dr. Richard Sparling and Dr. Sean McKenna for their thoughtfulness and many important suggestions throughout the course of my research. To our collaborators Dr. Ignacio Fita and Dr. Xavier Carpena in Barcelona for the crystallography. My sincere thanks to Mr. Terry James and Ms. Veronica Larmour for guiding me and teaching me about the FPLC instrument and giving me a constant encouragement to pursue the protein purification stages. Special mention to the FPLC machine which made my life much easier during the days of stress. Next, I would like to thank several graduate students and staffs of the Microbiology department with whom I had dealt with. Apart from the lab, I would like to thank god to whom I believe and to my family members in India.

TABLE OF CONTENTS

LIST OF FIGURES

LIST OF TABLES

LIST OF ABBREVIATIONS

A_{280}	Absorbance at 280 nanometers
Å	Angstrom
Amp	Ampicillin
AAA	ATP Associated with other cellular Activities
ATP	Adenosine Tri-Phosphate
bp(s)	Base pair(s)
C^o	degree Celsius
CBB	Coomassie Brilliant Blue
c-myc	Cellular myelocytomatosis
CV	Column volume
Da	Dalton
DEAE	Diethylaminoethyl
DMSO	Dimethylsulphoxide
DNA	De-oxyribonucleic acid
Dnm1p	Dynamin1 protein
DTT	Dithiothreitol
EDTA	Ethylenediaminetetraacetic Acid
E.coli	*Escherichia coli*
FPLC	Fast protein liquid chromatography
g	Gram
GTPase	Guanosine Triphophatase

His	Histidine
IPTG	Isopropyl β-D-thiogalactopyranoside
Kan	Kanamycin
kDa	kilo Dalton
kbp(s)	kilo base pair(s)
L	Litre
LB	Luria-Bertani
µL	Microlitre
µM	Micromolar
M	Molar
mAu	milli-Absorption Units
mg	Milligram
mL	Millilitre
mM	Millimolar
min	Minute
MW	Molecular weight
MWCO	Molecular weight cut-off
NADH	Nicotinamide adenine dinucleotide (oxidized)
NADPH	Nicotinamide adenine dinucleotide phosphate
ng	Nanogram
nm	Nanometer
O/N	Overnight
OD_{600}	Optical density at 600 nanometers
ORF	Open reading frame

PAGE	Polyacrylamide gel electrophoresis
PBS	Phosphate Buffered Saline
PCR	Polymerase chain reaction
PDB	Protein data bank
PEX	Peroxin
pM	Picomolar
psi	Pounds per square inch
PTS	Peroxisomal targeting sequence
RNA	Ribonucleic acid
rpm	Rotations per minute
SDS-PAGE	Sodium Dodecyl-phosphate Poly-Acrylamide Gel Electrophoresis
TAE	Tris-Acetate EDTA buffer
Tris	Tris (hydroxymethyl) aminomethane
U	Units
V	Volts
Vps1p	Vacuolar protein sorting protein 1
v/v	Volume per unit volume
w/v	Weight per unit volume

Do not look back and ask “WHY”? , look forward and ask “WHY NOT”?

----- Anonymous

1. INTRODUCTION

1.1 Peroxisome

1.1.1. Peroxisome: General Overview

Peroxisomes are ubiquitous and are considered to be vital organelles in eukaryotic cells. They were first observed by electron microscope in animal cells (1950) and later in plant cells (1960) (Purdue and Lazarow, 2001). Initially described as microbodies by Rhodin in 1954 (Rhodin, 1954), they were eventually named peroxisomes by de Duve and Baudhuin in 1966 (De Duve and Baudhuin, 1966) on the basis of the hydrogen peroxide metabolizing enzymes present in them.

Peroxisomes are single membrane cellular organelles which have variable granular composition and are roughly spherical with an average diameter of 0.2 to 1.7 µm (Wanders and Waterham, 2006) [Figure 1-1]. The protein content of peroxisomes varies across species, but the presence of proteins common to many species has been used to suggest an endosymbiotic origin; that is, peroxisomes evolved from bacteria that invaded larger cells as parasites, and very gradually evolved a symbiotic relationship (Gabaldon, 2010). During this process, the enzyme complement of the peroxisomes diverged among different hosts. Degradation of hydrogen peroxide and breakdown of fatty acids are two functions common to yeast and human peroxisomes (Alberts B et al., 2002). In fact, yeast mitochondria lack the enzymes for beta-oxidation, making the peroxisomes the primary site of fatty acid degradation (Kunau et al., 1995). Enzymes for the catabolism of D-amino acids and polyamines, for the biosynthesis of plasmalogens and ether phospholipids also exist. Yeast peroxisomal enzymes are also involved in the

biosynthesis of lysine, the glyoxalate shunt, the degradation of amino acids and methanol and the oxidative utilization of specific carbon and nitrogen sources (Corpas et al., 1992). In plants, peroxisomes are involved in photorespiration (Cooper and Sunderland, 2000).

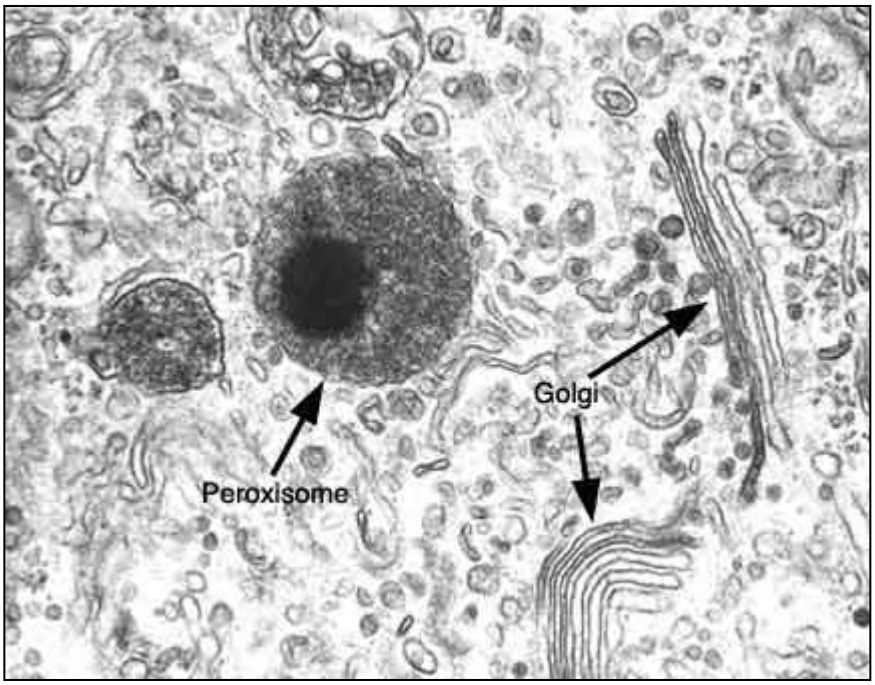

Figure 1-1: Electron micrograph of yeast peroxisomes; A transmission electron micrograph of a cross section of a yeast cell showing the peroxisome and golgi bodies.

1.1.2. Peroxisomal Biogenesis

Unlike the mitochondria and chloroplast, which contain their own rudimentary genome, peroxisomes, do not contain a genome of their own, and they lack a protein secretory apparatus (Hettema and Motley, 2009). Lacking both DNA and ribosomes, peroxisomes must therefore import all proteins required for their structure and function as an integral part of their biogenesis or assembly (Lazarow, 2003).

The early stages of peroxisome biogenesis have been a subject of much controversy. A longstanding concept proposed that peroxisomes are autonomous organelles derived from pre-existing ones by division with the help of peroxisomal membrane proteins and matrix protein import, and subsequent fission to form enlarged organelles (Tabak et al., 2006). Moreover, two proteins GTPases Vps1p and Dnm1p which are required for mitochondrial fission and vacuolar sorting, also assemble on the cytoplasmic face of the peroxisomal membrane at sites where division will occur, therefore participating in endocytosis and regulating peroxisome abundance (Rooij et al., 2010; Mozdy et al.. 2000). An alternative view is that peroxisomes are formed by the *de novo* synthesis from the endoplasmic reticulum where the division process has been suggested to occur at an endoplasmic reticulum (ER) sub domain before the maturation pathways (Rachubinski et al., 2001). Several subsets of membrane and matrix proteins are needed during its maturation phase. Recent studies have shown that it seems more likely that *de novo* formation of peroxisomes represents an alternative system of peroxisomal propagation in cells where these fission proteins are absent (Schrader and Fahimi, 2006) [Figure 1-2].

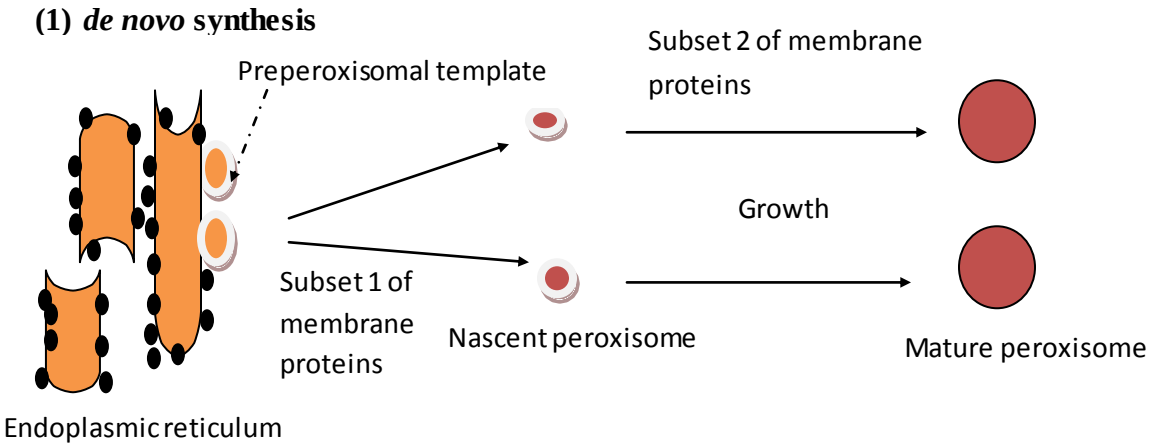

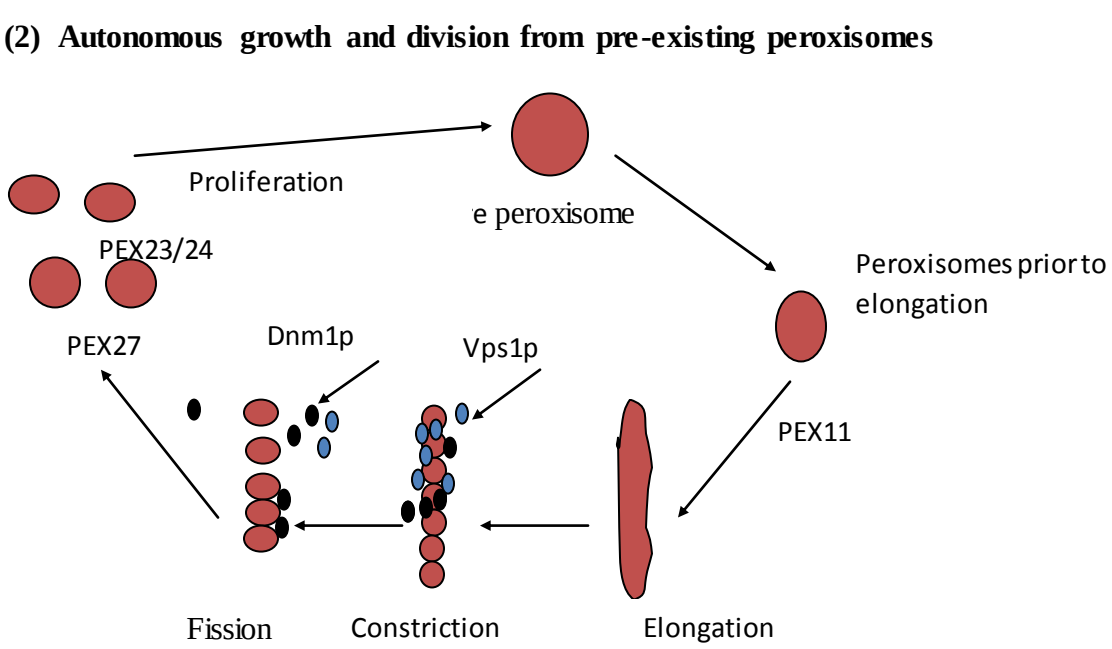

Figure 1-2: **Two models of peroxisomal biogenesis;** Two models for peroxisome biogenesis are outlined in the above figure. **(1)** In *de novo* synthesis of peroxisomal biogenesis, the preperoxisomal membrane templates are formed from the rough endoplasmic reticulum and are transformed into nascent peroxisomes with the help of a subset of peroxins PEX16 and PEX25. These nascent peroxisomes then undergo growth and division with the help of another subset of peroxins PEX23, PEX24, PEX31 (Tabak et al., 2006), **(2)** in another model, the peroxisomes are thought to be formed from the pre-existing mature peroxisomes. PEX11 helps peroxisomes to elongate before constriction. GTPase proteins Vps1 allows constriction while Dnm1 helps in fission, and PEX27 helps in distribution to the daughter cells. Ultimately, PEX23 and PEX24 are needed for proliferation to form mature peroxisomes (Schrader and Fahimi, 2006).

1.2 Biogenesis of Yeast Peroxisome

A group of protein factors referred to as peroxins which are encoded by the PEX genes are integral to the biogenesis of the yeast peroxisome. At present, over 30 different PEX proteins are known, some being conserved among all species and some lacking mammalian homologs (Table 1). These peroxisomal proteins are synthesized on the free poly-ribosomes and are imported post-translationally from the cytoplasm to the peroxisome utilizing the Peroxisome Targeting Signal sequences (PTS) (Stephen and Cynthia, 2002).

1.2.1. Matrix Protein Import

Matrix protein import involves four distinct steps: (1) recognition of the protein by receptor, (2) docking of the receptor protein complex on the membrane, (3) membrane translocation of the receptor-protein complex, and (4) receptor recycling (Stephen and Cynthia, 2002). A diagram of the general pathway of peroxisomal biogenesis is shown in Figure 1-3.

1.2.2. Peroxisomal Targeting Signal Sequences and Receptor peroxins

Two consensus motifs PTS1 and PTS2 have been identified in different organisms. PTS1 is present at the carboxy-terminus of most matrix proteins commonly involving the tripeptides S-K-L or more variable S (C/A)-K(R/H)-L (Hettema et al., 1999). However, recent studies about this motif have shown considerable variation with respect to its length and the specificity of the signal may also differ between species (Subramani et al., 2002). The second or PTS2 signal sequence is a nonapeptide (R/K)-(L/V/I)-X_5 - (Q/H)-(L/A) located in the first 20 residues at the N-terminus (Braverman et

al., 1997). PEX5 is the soluble receptor for proteins bearing a PTS1. The amino-terminal half is involved in a number of protein-protein interactions while the tetratricopeptide repeats (TPR) present in the carboxy-terminal are responsible for binding PTS1 (Hettema et al., 1999). PEX7 with Trp-Asp repeats binds to PTS2-containing proteins. In yeast, PTS2 targeting requires accessory proteins of the PEX20 family. Moreover, the PEX7 receptor protein requires accessory protein factors such as PEX18 and PEX21 for its functioning (Braverman et al., 1997) but in mammals, PEX7 binds to the longer form of the two splicing variants of PEX5 making PTS2 import dependent on PEX5 (Paul et al., 2005).

1.2.3. Docking of the receptor protein complex on the membrane

The receptor bound protein binds to a docking complex in the peroxisomal membrane formed by various peroxins including PEX13, PEX14 and PEX17. While PEX17 is found tightly associated with the periphery of the membrane, PEX13 is an integral membrane protein which has a SRC Homology 3 (SH3) domain cytosolically oriented at its C terminus. The SH3 domain has a characteristic beta-barrel fold which consists of five or six β-strands arranged as two tightly packed anti-parallel β sheets (Pawson, 1993). This domain mediates separate binding sites for PEX5 and type II SH3 ligand PEX14. In addition, two well conserved hydrophobic residues of yeast PEX14 in a W-X-X-X-F(Y) motif are responsible for its binding to receptor PEX5. The localization of the N terminal of PEX14 is yet to be determined, although it is thought to be residing in the cytoplasm (Paul et al., 2005). The interaction domain of PEX7 responsible for binding to PEX13 has been mapped only approximately to the N-terminal one hundred residues, to which other peroxins like PEX18 and PEX21 bind (Leon and Goodman,

2006). All of these PEX proteins work in a consortium for the proper docking of the peroxisomal membranes. However, the detailed understanding of the entire process is still lacking.

1.2.4. Membrane translocation of receptor-protein complex

Following their docking on the peroxisomal membrane, both PTS1 and PTS2 receptor-protein complexes are translocated in a process involving the integral membrane proteins PEX2, PEX10 and PEX12 containing 'RING finger' domains exposed to the cytosol (Baker et al., 2010). PEX8 interacts with the RING finger motifs of these proteins to organize or stabilize the larger protein transport complex (Agne et al., 2003). As yet, it is not known if a transmembrane proton or ion gradient is coupled to protein transport, but energy released by ATP hydrolysis is required with PEX1 and PEX6 acting as ATPases for release of the receptor proteins (see below) (Erdmann and Schliebs, 2005).

1.2.5. Receptor recycling

PTS1 and PTS2 bind the peroxisomal proteins which are then delivered to the membrane without directly entering into the organelle (Dodt et al., 1996). However, recent studies in yeast and mammals support an ‘extended shuttle’ mechanism, in which the receptors enter the peroxisome together with their cargo, release the cargo in the lumen of the peroxisome and are then recycled back to the cytosol to participate in further rounds of import. The details of the recycling mechanism are still under debate (Erdmann and Schliebs, 2005).

After delivering their transported proteins to the membrane complex, PEX5 and PEX7 are released and return to the cytosol for the next round of import. PEX1 and PEX6

interact with the protein-receptor complex in an ATP-dependent manner and the energy released in ATP hydrolysis facilitates release of the PTS1 receptor PEX5 into the cytosol (Dodt et al., 1996). In yeast, PEX1 and PEX6 are anchored by a phosphorylated tail anchored type II integral membrane protein PEX15 (Elgersma et al., 1997). In addition, PEX26 anchors PEX1 and PEX6 to peroxisome membranes, possibly to form heteromeric AAA ATPase complexes required for the recycling of the receptor PEX5 from the peroxisomal membrane to the cytosol (Matsumoto et al., 2003). In contrast, the mechanism underlying the recycling of PEX7 receptor is still unknown (Nishimura et al., 2009).

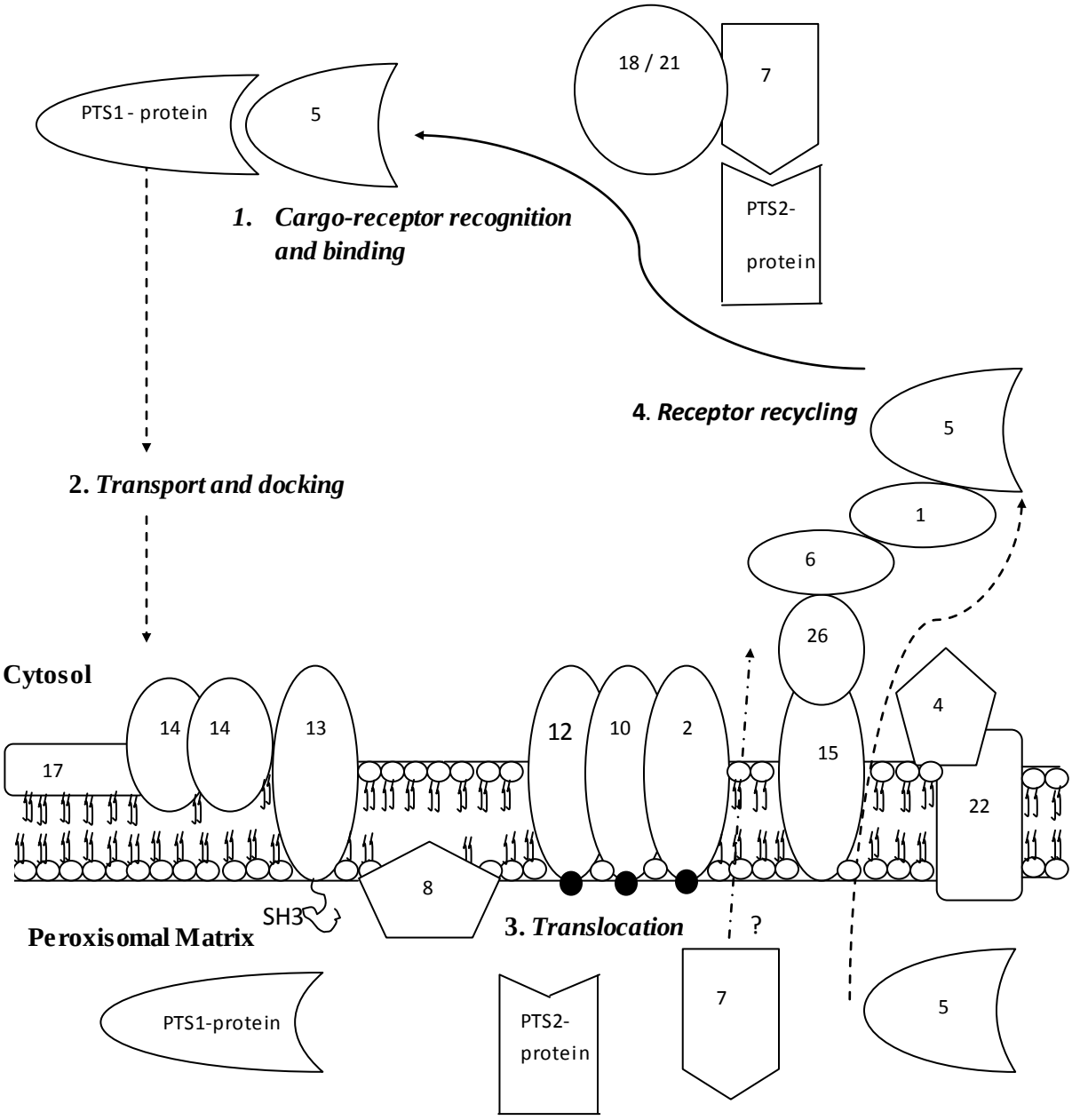

Figure 1-3: General model of peroxisomal matrix protein import; The above figure shows the generalized model for peroxisomal matrix protein import which follows several steps, **1**. The receptors such as PEX5 and PEX7 recognize the PTS1 and PTS2 signal bearing peroxisomal proteins respectively and bind tightly to each of their cognate partners. PTS1 is present at the carboxy-terminus of most matrix proteins while PTS2 is present at the amino-terminus. PEX18 and PEX21 binds to PEX7 to form an import-competent complex which then binds to PTS2 signal sequences, **2.** The receptor-protein pair is then transported from the cytosol towards the peroxisomal membrane where the

actual docking takes place. PEX13, PEX14 and PEX17 help in the docking. The mode of action of PEX14 and PEX17 is yet to be determined. The SH3 domain of PEX13 mediates separate binding sites for PEX5; however the binding of PEX7 to PEX13 is still unknown, **3.** The translocation of both PTS1 and PTS2 receptor-protein complexes are translocated in a process involving the integral membrane proteins PEX2, PEX10 and PEX12 containing 'RING finger' domains exposed to the cytosol (shown in solid black). PEX8 interacts with the RING finger motifs of these proteins to organize or stabilize the larger protein transport complex. However, it is still not known if a transmembrane proton or ion gradient is coupled to protein transport, **4.** PEX1 and PEX6 interact with the protein-receptor complex in an ATP-dependent manner and the energy released in ATP hydrolysis facilitates release of the PTS1 receptor PEX5 into the cytosol for the next round of import, however, PEX7 receptor recycling is still unknown. PEX6-PEX1 complex is anchored by PEX15/PEX26 to the peroxisomal membrane.PEX4 helps in PEX5 ubiquitination and is anchored on the membrane by PEX22. (Small empty circles represent polar head groups and lines represent hydrophobic phospholipid tails of the membrane).

Table 1-1: Proteins implicated in the biogenesis of peroxisomes

Peroxin	Organisms	Localization	Proposed function
PEX1	m, p, f, y	cytosol/membrane	Matrix protein import, export of PEX5
PEX2	m, p, f, y	membrane	Matrix protein import, translocation
PEX3	m, p, f, y	membrane	Membrane biogenesis, PMP import
PEX4	p, f, y	cytosol/membrane	Matrix protein import, PEX5 ubiquitination.
PEX5	m, p, f, y	cytosol/membrane	Matrix protein import, PTS1 (& PTS2 in m, p)
PEX6	m, p, f, y	cytosol/membrane	Matrix protein import, export of PEX5 receptor.
PEX7	m, p, f, y	cytosol/membrane	Matrix protein import, PTS2 receptor
PEX8	p, f, y	matrix/membrane	Matrix protein import
PEX10	m, p, f, y	membrane	Matrix protein import, translocation
PEX11	m, p, f, y	membrane	Division and proliferation
PEX12	m, p, f, y	membrane	Matrix protein import, translocation
PEX13	m, p, f, y	membrane	Matrix protein import, docking
PEX14	m, p, f, y	membrane	Matrix protein import, docking
PEX15	*Sc*	membrane	Matrix protein import, PEX6 anchor.

PEX16	m, p, f, *Yl*	membrane	Membrane biogenesis
PEX17	y	membrane	Matrix protein import, docking
PEX18	*Sc*	cytosol/membrane	Matrix protein import, PTS2 import
PEX19	m, p, f, y	cytosol/membrane	Membrane biogenesis, PMP import
PEX20	f, y	cytosol/membrane	Matrix protein import, PTS2 import
PEX21	*Sc*	cytosol/membrane	Matrix protein import, PTS2 import
PEX22	p, f, y	membrane	Matrix protein import, PEX4 anchor
PEX23	f, y	membrane	Proliferation
PEX24	f, y	membrane	Proliferation
PEX25	y	membrane	Proliferation
PEX26	m, f, y	membrane	Matrix protein import, PEX1/PEX6
PEX27	*Sc*	membrane	Proliferation
PEX28	*Sc*	membrane	Proliferation (PEX24 ortholog)
PEX29	y	membrane	Proliferation
PEX30	*Sc*	membrane	Proliferation (PEX23 ortholog)
PEX31	*Sc*	membrane	Proliferation
PEX32	y	membrane	Proliferation

m = mammals; p = plants; f = filamentous fungi; y = yeasts; *Yl*, *Yarrowia lipolytica* only; *Sc*, *Saccharomyces cerevisiae* only.

1.3. Metabolic importance of the peroxisome

The importance of the metabolic activities supported by the peroxisome is evident in the metabolic diseases associated with mutations in peroxisomal genes which can be categorized in three groups: peroxisome biogenesis disorders, peroxisomal multi-enzyme disorders and peroxisomal single-enzyme disorders (Gould and Raymond, 2001).

The peroxisome biogenesis disorders (PBDs) are diseases in which the entire process of peroxisomal assembly has malfunctioned, and nearly all normal peroxisomal functions are either absent or deficient. Sometimes, this means that the peroxisomes themselves fail to form, or fail to form in sufficient numbers; other times "ghost peroxisomes" form, having somewhat the appearance of the real thing, but lacking the matrix enzymes necessary to function (Gould and Raymond, 2001; Wanders et al., 1995). Defects in PEX6 are the cause of peroxisome biogenesis disorder complementation group 4 (PBD-CG4) which refers to a group of peroxisomal disorders like Zellweger syndrome arising from a failure of protein import into the peroxisomal membrane or matrix (Braverman et al., 1995).

Peroxisomal multi-enzyme disorders are diseases in which several of the proteins necessary to peroxisomal function are lacking, but there is not a global loss of function as in the PBDs (Schutgens et al., 1986). Mutations in PEX18 and PEX21 are responsible for improper localization of PTS2 signal protein thiolase which is an important enzyme for β-oxidation.

Peroxisomal single-enzyme disorders are disorders in which the peroxisome is intact and functioning, except that there is a defect in just one enzymatic process, resulting in just one primary biochemical abnormality (Mannaerts and van Veldhoven,

1990). It doesn't necessarily follow that these diseases are any less severe than the PBDs; the loss of even a single peroxisome function is sufficient to cause disease that can closely mimic the PBDs and is every bit as severe. Mutation in *idp3* gene results in the improper functioning of IDP3 which leads to growth defects when cultured on media having unsaturated fatty acids (Singh et al., 1997).

Elucidation of the structures of all peroxisomal proteins which is the ultimate goal of the project will provide insight into the function of this important and interesting group of enzymes. Factors important in the biogenesis of the organelle, targeting and transport of proteins into the peroxisome and the catalytic function of the enzymes will be identified. This will lead to a better understanding of the development and maintenance of organelles in eukaryotic cells and may ultimately lead to solutions for metabolic diseases caused by peroxisomal malfunction.

1.4. Peroxisomal proteins chosen for this work

The long term goal of the research is to determine the structure of all peroxisomal proteins. For the work described in this thesis, a subset of peroxisomal proteins was chosen including both enzymes and peroxins. Specifically, the enzyme IDP3 and the peroxins PEX18, PEX21 and PEX6 were chosen**.**

1.4.1. Isocitrate Dehydogenase (IDP3)

Peroxisomes contain a complement of enzymes required for metabolic pathways that differ depending on cell type, developmental stage and food supply (Tolbert, 1981; van den Bosch et al., 1992). One of the most commonly distributed pathways in peroxisomes is that of fatty acid oxidation which is nearly ubiquitous in eukaryotic cells.

Mitochondrial β-oxidation on the other hand is restricted to mammalian cells and a few protists (Schulz-Borchard, 1988; Hashimoto, 1982). By contrast in fungi, fatty acid degradation is restricted to the peroxisome and growth on fatty acids results in proliferation of peroxisomes accompanied by a massive induction of peroxisomal proteins including the β-oxidation enzymes (Veenhuis, 1987).

The presence of double bonds in unsaturated fatty acids interferes with normal β-oxidation and requires specific attention to allow complete degradation of the fatty acid. This is accomplished in peroxisomes by the import of Δ^2 and Δ^3-enoyl-CoA isomerases and a NADPH-dependent 2, 4-dienoyl-CoA reductase (Kunau et al., 1995) found in all peroxisomes. The latter reductase is part of a novel pathway involving the successive reduction and isomerization of double bonds that results in the formation of intermediates that re-enter the β-oxidation pathway. The NADPH required by the NADPH-dependent reductase may be provided by any dehydrogase including β -ketoacyl-CoA dehydrogenase (part of the β-oxidation pathway) and isocitrate dehydrogenase (see below).

The existence of isocitrate dehydrogenase in peroxisomes was determined in oleic acid-induced *S. cerevisiae* from which proteins were fractionated and sequenced, allowing the synthesis of DNA fragments for gene cloning resulting in identification of an ORF later named YNL009W (Henke et al., 1998). The gene had 68% and 70% identity with IDP1 and IDP2, respectively, leading to its identification as IDP3 (Haselbeck et al., 1991; Hall et al., 1994). The mitochondrial $NADP^+$-dependent isocitrate dehydrogenase with 70% identical sequence has had its structure determined (Peng et al., 2008) [Fig. 1-4].

Subsequent immunoblot assay of fractionated cellular components revealed that IDP3 was localized exclusively in the peroxisomal fractions. Furthermore, Δ*idp3* mutants lacked the enzymatic activity (Qian et al., 2010). Amino acids C-K-L at the C-terminus of IDP3 identify it as a probable PTS1-targeted protein (Gould et al., 1987 and Elgersma et al., 1996) and this was confirmed in the Δ*idp3* CKL mutant where the truncated IDP3 was found only in the cytosolic fractions.

A role for isocitrate dehydrogenase in the TCA cycle is clear, but a role in fatty acid metabolism is not so obvious. Growth experiments provided some direction when the Δ*idp3* mutant was found to grow on media containing glucose, glycerol or stearic acid, but not oleic acid. Stearic acid and oleic acid are both C18 fatty acids differing only in the presence of one double bond in oleic acid (Δ^9). The implication was that IDP3 must be playing a role in the conversion of the unsaturated fatty acid into an intermediate in the β-oxidation pathway. Similarly, the Δ*idp3* mutant would not grow on the Δ^6 unsaturated fatty acid petroselinic acid unless complemented by the wild type *idp3* (Henke et al., 1998).

Isocitrate dehydrogenase catalyzes the conversion of isocitrate to α-ketoglutarate with coincident production of NADPH.

$$\text{Isocitrate} + NADP^+ \rightarrow \alpha\text{-ketoglutarate} + NADPH + H^+ + CO_2$$

Clearly α-ketoglutarate does not have a role in fatty acid degradation, so it is more likely the product NADPH which is important. Normally the enoyl-CoA isomerase would isomerize the cis Δ^3 double bond to trans Δ^2 for continuation of unsaturated fatty acid synthesis, but this would not require NADPH. This seems to imply that an alternate

pathway involving a NADPH-dependent reductase step is involved in oleic acid metabolism, but whether this involves a side reaction of the NADPH-dependent dienoyl-CoA reductase or another as yet uncharacterized enzyme remains unclear.

It has been well established that IDP3 plays a vital role in peroxisomal metabolism. In the cytosol, NADPH is generated by several biochemical pathways like the pentose phosphate pathway. However, because of the impermeability of the peroxisomal membrane for pyrimidine nucleotides, the cytosolic NADPH pool cannot directly account for the peroxisomal need for NADPH. This emphasizes the necessity for an NADPH regenerating system in the peroxisomal lumen where IDP3 generates NADPH which in turn is needed by the peroxisomal enzymes to degrade unsaturated fatty acids (van Roermund et al., 1995)

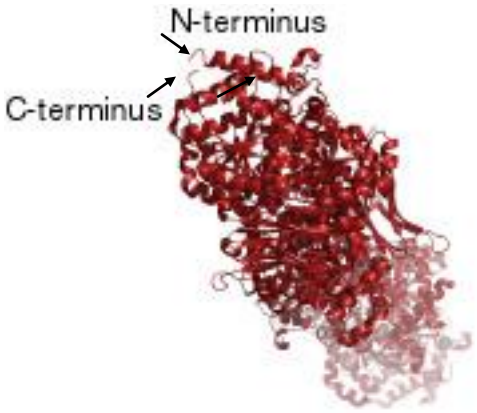

Figure 1-4: Cartoon representation of *Saccharomyces cerevesiae* mitochondrial NADP$^+$-dependent isocitrate dehydrogenase; Structure of *Saccharomyces cerevesiae* mitochondrial NADP$^+$-dependent isocitrate dehydrogenase (PBD accession number: 2QFW), oriented to illustrate both N- and C- termini.

1.4.2. PEX18 and PEX21

While PEX7 directly recognizes the PTS2 signal sequence, a complex of the PEX7-protein pair with either PEX18 or PEX21 is required for delivery of the protein to the membrane docking complex of PEX13 and PEX14 (Sowinski et al., 2001). This role is most clearly defined by the evidence that import of PTS2-targeted thiolase is abolished in cells lacking PEX18 and PEX21. By contrast, the import of PTS1-targetted proteins and acyl-CoA oxidase which is neither PTS1 nor PTS2-targetted is normal. In addition, screening peroxisomal fractions for protease sensitivity revealed that PEX18 and PEX21 were readily cleaved whereas thiolase (a matrix protein) was not cleaved until detergent was added to disrupt the membrane. Thus, both proteins are situated primarily in the cytosol outside the peroxisome (Katharina et al., 2002). The interaction of both proteins with PEX13 was confirmed in a yeast two-hybrid assay (Barnett et al., 2000).

The redundant nature of PEX18 and PEX21 was demonstrated in a simple growth experiment where individual Δ*pex18* and Δ*pex21* mutants grew at near wild type rates (Δ*pex21*) or slightly slower (Δ*pex18*), whereas the double mutant did not grow at all. The direct determination of thiolase transport in these mutants revealed normal transport in Δ*pex21*, only 50% transport in Δ*pex18* and no transport in the double mutant. Thus, while one or the other of PEX18 or PEX21 is essential for the transport of PTS2 targeted proteins into the peroxisome, their roles are entirely redundant (Purdue and Lazarow, 1998). It remains to be determined why PEX18 appears to have a more important role than PEX21.

Sequence comparison of the similar sized PEX18 and PEX21 reveals a weak 23% identity overall but a slightly higher 35% identify in the C-terminal 60 amino acids. This

suggested that it is the C-terminus that is involved in the interaction with PEX7, consistent with the sequence being present in all *pex18* and *pex21* library clones isolated with PEX7 bait using immunocoprecipitation in an *in vitro* binding assay (Katharina et al., 2002). No other sequence homologues of either protein have been reported.

A myc tag is a polypeptide tag derived from the c-*myc* gene that can be added to a protein and is used in different subcellular localization studies that require recognition by an antibody (Terpe, 2003). In the absence of functional docking or translocation machinery, immunoprecipitates of myc tagged PEX7 contain a drastically increased amount of the PTS2 protein, thiolase, as a result of cytosolic accumulation in these mutants. PEX18 and PEX21 mediate the docking of thiolase to the docking complex, PEX13 and PEX14 and if this is correct, such an apparent accumulation of cargo-loaded receptor should also occur in a Δ*pex18*Δ*pex21* strain. The myc tagged PEX7 immunoprecipitates of a wild-type strain contained very small amounts of thiolase, as expected, whereas those of *pex13* and *pex14* mutant strains showed an accumulation of thiolase. Moreover, when the amount of coimmunoprecipitated thiolase in a Δ*pex14*Δ*pex18*Δ*pex21* triple-mutant strain was compared to those of the Δ*pex14*, Δ*pex18*, Δ*pex21*, and wild-type strains, no thiolase accumulated in the triple mutant. This result indicates that the accumulation of the PEX7-thiolase complex in the Δ*pex*14 strain is dependent on PEX18 and PEX21 which is required in the import process prior to PEX14. Thus, PEX18 and PEX21 probably act to promote the formation of an import competent PTS2 substrate complex that precedes docking of PEX7 to the membrane (Katharina et al., 2002).

PEX18 and PEX21 are constantly degraded in the cytosol due to ubiquitination which is not evident for the fraction of peroxisomally localized PEX18 and PEX21 (Purdue and Lazarow, 2001). Whether this protein degradation of these proteins has a part in the physiological relevance of the PTS2 dependent protein import or to any other step that follows docking is yet to be determined.

1.4.3. PEX6

As described above, peroxisomal proteins are synthesized on free ribosomes and transported into the peroxisome post-translationally. Specifically, PEX5 and PEX7 bind to proteins containing recognition sequences PTS1 or PTS2 and work with a membrane bound system to shuttle the proteins across the membrane (Paul et al., 2005). The transport process requires energy derived from ATP hydrolysis. PEX6 encoded by the *pex6* gene is one of two ATPases involved. PEX1 and PEX6 are members of the AAA (ATPase Associated with other Activities) family of ATPases, a large superfamily of proteins involved in the ATP-dependent rearrangement of protein complexes. All members of the AAA family contain one or two AAA-cassettes, comprising about 230 amino acids and are characterized by Walker A and Walker B motifs for ATP-binding and ATP-hydrolysis respectively (Erdmann and Schliebs, 2010). They are essential for many activities like cell cycle function, vesicular transport, mitochondrial functions and proteolysis. To fulfill their role in peroxisome biogenesis (Ogura and Wilkinson, 2001), there is a direct association between PEX1 and PEX6 suggesting that they work cooperatively and are non-redundant (Keil et al., 1999).

According to the predicted domain structure, the PEX6 sequence was divided into three parts: the N-terminal region (N, amino acid 1– 400), the first AAA-cassette (D1, amino acid 394 – 681) and the second AAA cassette (D2, amino acid 669 –1043) (Beyer, 1997; Erdmann et al., 1991). Proteins of known structure with sequence similarity to the *Saccharomyces cerevisiae* protein PEX6 were identified by comparing yeast protein sequences against protein sequences in the RCSB Protein Databank (PDB) using the Smith-Waterman analysis program. There were 36 homologs found for this yeast protein out of which a protein named AAA ATPase p97 of *mus musculus* (44% identical, 30% similar) showed the highest sequence similarity. Figure 1-5 shows the cartoon representation of the structure of murine AAA-ATPase p97 (Zhang et al., 2000).

PEX6-dependent recycling of PEX5 from the peroxisomal compartment back to the cytosol was established by an *in vitro* export assay. When the membranes were incubated with the cytosol from a Δ*pex6* strain, there was no effect on the distribution of Ubiquinated (Ub) - PEX5, whereas incubation with wild-type cytosol resulted in the disappearance of the ubiquitinated PEX5 species from the organellar fraction. Moreover, this protein did not appear in the supernatant which led to the assumption that it had been removed from the membrane in an AAA-peroxin-dependent manner and finally degraded. To investigate whether the previously reported ATP dependence of the PEX5 export step is also maintained in the *in vitro* export assay, the same experiment was repeated in the absence of an ATP-regenerating system. Retention of Ub-PEX5 in the organellar pellet confirmed that PEX6 was involved in the recycling of PEX5 from the peroxisomal membrane into the cytosol for next round of import (Birschmann et al., 2005).

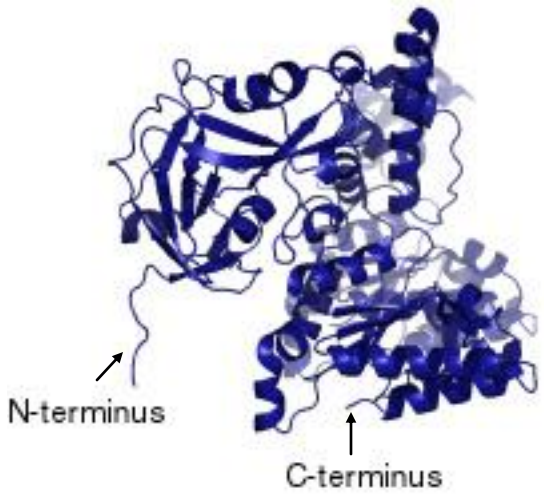

Figure 1-5: Cartoon representation of the structure of the murine AAA ATPase p97; Structure of murine AAA ATPase p97 (PBD accession number: 1R7R), oriented to illustrate both N- and C- termini.

1.5. Objective of the work described in the thesis

The objective of the work described in this thesis is to purify, crystallize and solve the structure of *S.cerevisiae* peroxisomal proteins IDP3, PEX18, PEX21 and PEX6.

2. MATERIALS AND METHODS

2.1. Biochemicals and common reagents

The biochemicals and reagents, unless otherwise stated, were purchased from Fisher Scientific Ltd. (Mississauga, Ontario) and Sigma Chemical Co. (St. Louis, Missouri). Restriction enzymes and buffers, PCR reaction kits, T4 DNA ligase were purchased from Invitrogen Canada Inc. (Burlington, Ontario). MilliQ water (Millipore Co., Billerica, Massachusetts) was used to prepare solutions and growth media.

2.2. Bacterial strains

The *E. coli* strains and plasmids used in this study are listed in Table 2-1. *E. coli* BL21 (λDE3) has genome-encoded T7 RNA polymerase which is under the control of the lacUV5 promoter. IPTG, which acts as a substrate analogue of lactose, was used to activate lacUV5 promoter to produce mRNA encoding the recombinant protein. Because this strain is also *endA* deficient, it lacks the endonuclease that degrades plasmid DNA in many miniprep methods.

2.3. LB media and storage media

E. coli cultures were grown in the LB medium consisting of 10 g of Tryptone, 5 g of yeast extract and 5 g of NaCl per litre of culture. Likewise, solid LB plates contained the same ingredients supplemented with 10 g/L of agar. Bacterial stock cultures were stored in 24% DMSO or in 30% glycerol at -60 ^{o}C for future experiments. For large scale protein expression, 500 mL of expression media consisting of 2.5 g of NaCl, 2.5 g of Yeast extract (Difco) and 5 g of Tryptone (Difco) were prepared.

Table 2-1: Genotype and sources of *Escherichia coli* strains and plasmids used in this study.

	Genotype	Source
***E. coli* strains**		
NM522	*supE Δ (lac-proAB) hsd-5* [*F' proAB* lac^q *lacZΔ15*]	Mead et al., 1985.
JM109	*recA 1 supE44 endA 1 hsdA 1 hadR 17 gyrA96 relA 1 thi Δ (lac-proAB)*	Yanisch-Perron et al. 1985.
BL21	F^- *ompT gal dcm lon* $hsdS_B$ (r_B^- m_B^-) *λ (DE3) pLysS* (cm^R)	Davanloo et al., 1984.
BL21 Rosetta	F^- *ompT* $hsdS_B$ (R_B^- m_B^-) *gal dcm λ (DE3) [lacI lacUV5-T7 gene 1 ind1 sam7 nin5]* pLysS RARE (Cam^R)	Novagen
Plasmids		
pKS-	Amp^R	Stratagene
pET28b	Kan^R	Novagen

2.4. Antibiotic concentration in the growth media

For plasmids encoding an ampicillin resistance gene, ampicillin was added to the liquid and solid media to a concentration of 100 µg/mL. For plasmid carrying the kanamycin resistance gene, the antibiotic was added to solid and liquid media to a concentration of 40 µg/mL.

2.5. Plasmid DNA isolation and cloning

2.5.1. DNA isolation

The plasmids harbouring the genes of interest (i.e. *pex6, pex18, pex21, idp3, sym1* and *ant1*) were obtained cloned into the plasmid pBG1805 (Grayhack et al., 1999) transformed in *E. coli* DH5α. These strains were inoculated in 5 mL LB medium in the presence of an appropriate concentration of ampicillin and incubated overnight at 37 ^{o}C. 3 mL of cells were spun down using the bench top ultracentrifuge (IEC Micro MB) and the supernatant was discarded. The plasmids were isolated according to Sambrook et al. (1989). The bacterial pellet was resuspended in 200 µL of glucose-EDTA-RNase buffer (25 mM Tris-HCl, pH 8.0, 1% glucose, 10 mM Na-EDTA, and 0.35 mg/mL RNase). The cells were lysed in lysis buffer (1% SDS and 0.2 M NaOH). After incubating for 10 minutes, 300 µL of 6.3 M ammonium acetate was added and the mixture was centrifuged twice to remove all precipitate. Addition of 550 µL of isopropanol precipitated the plasmid DNA. After a 15 minute incubation, plasmid DNA was pelleted by centrifugation, washed twice with 70% ethanol, and dried in a vacuum chamber. The DNA pellet was either resuspended in water or TE buffer (10 mM Tris, pH 8.0, 1 mM Na-EDTA) and kept at -20 ^{o}C.

2.5.2. PCR amplification

The primers outlined in Table 2.2 were purchased from Invitrogen Inc. Canada and dissolved initially in 20 µL of DNase-RNase free water and then diluted to 40 pM before storage at -20 ^{o}C. A DNA Thermal cycler from Perkin Elmer Cetus Company was used for all amplifications including 1 X PCR buffer (20 mM Tris-HCl, pH 8.4, 50 mM KCl), 0.2 mM dNTPs, 1.5 mM $MgCl_2$, 0.5 µM of both forward and reverse primers, 1 µg of plasmid DNA, and 2.5 units of *Pfu* DNA polymerase. Autoclaved water was used to make up for the volume to 100 µl. 50 µl of light mineral oil was added to the top of the reaction mixture to prevent evaporation. The reactions normally involved 35 cycles of denaturation at 98 ^{o}C for 45 sec, primer annealing at 50 - 55 ^{o}C for 30 sec and primer extension at 68 to 72 ^{o}C for 90 sec. The final elongation was at 72 ^{o}C for 5 min after which the mixture was kept at 4 ^{o}C until separation. Some variation in conditions including annealing temperatures and [$MgCl_2$] were required for optimum amplification of different genes.

Table 2-2: Oligonucleotide primers used for PCR amplification

ORF	Primer	Oligonucleotide sequence
YNL329C	PEX6-F	GCAGGGTCGACA**ATGAAGGCATCGCT**
	PEX6-R	ACAAGGCGGCCGCTTA**AGCACCTTCAAAA**
YHR160C	PEX18-F	GCAGGGAGCTCA**ATGAATAGTAACCGA**
	PEX18-R	AAGAACTCGAGTTA**AGCAATTCTGTC**
	PEX18-C' His	AAGAAAGCTGGCTCGAGAATTCTGTC
YGR239C	PEX21-F	AGCAAAGCTTCAT**ATGCCCAGTGTCTG**
	PEX21-R	AAGAAAGGATCCTTA**ATCAAGTATGTC**
	PEX21-C' His	AAGAAAGCTGGGTGGATCCAGTATGTC
YNL099W	IDP3-F	GCAGGGGATCCA**ATGAGTAAAATTAA**
	IDP3-R	AAGAAAAGCTTTTA**TAGTTTGCACAT**

Note: Sequence in bold represents the start (forward) and end (reverse) of the ORF

2.5.3. Agarose Gel Electrophoresis and purification

From the amplified reaction mixture, 10 µL was mixed with 3 µL of stop buffer (40% glycerol, 10 mM EDTA, pH 8.0, 0.25% bromophenol blue) and loaded on an Agarose gel (1% w/v Agarose in 40 mL of 50 mM TAE buffer (50 mM Tris-Acetate pH 8.0, 1 mM EDTA, 1 µg/mL ethidium bromide). Agarose gels were cast in Bio-Rad Mini Sub Cell Plexiglass horizontal electrophoresis trays (6.5 cm x 10 cm). 1 Kb Plus™ DNA Ladder purchased from Invitrogen Inc., Canada was used throughout as the reference for all the DNA electrophoresis experiments. Electrophoresis was performed at a constant current of 48 milliamps for 45 to 60 minutes in TAE buffer until the bromophenol blue dye marker front had migrated approximately two-thirds the length of the gel. DNA bands were visualized with ultraviolet light using a gel documentation system (FluorChem™ from Alpha Innotech). Agarose segments containing DNA bands of the appropriate size were excised and the DNA extracted from the Agarose were purified using the UltraClean kit (MO BIO Laboratories Inc.).

2.5.4. Cloning of gene fragments

The purified insert and pKS- vector DNA samples were subjected to restriction digestion with the appropriate restriction enzymes (Table 2-3) and buffers for 3 or more hours at 37 ^{o}C, separated on Agarose gels and purified using the gene clean kit (see above). Ligation of DNA fragments was carried out according to the procedure of Sambrook et al. (1989). Insert and vector DNA samples were mixed with 2 µL of ligase buffer (250 mM Tris-HCl, pH 7.6, 50 mM $MgCl_2$, 5 mM ATP, 5 mM DTT, 25% (w/v) polyethylene glycol-8000) in a final volume of 10 µL. After adding 1 unit of T4 DNA

ligase, the mixtures were incubated at 16 ^{o}C for 15 hours. Usually three or four ligation mixtures containing a range of insert DNA concentrations were set up at the same time.

E. coli NM522 was grown in LB medium to an OD_{600} value between 0.4 and 0.6 at 37 ^{o}C pelleted and cooled on ice. After the addition of 0.1 M $CaCl_2$, the cells were incubated 30 min on ice, before being divided into 100 µL volumes to which the ligation mixtures were added. After 30 minute incubation on ice for transformation, the cell suspension was heat shocked for 105 sec at 42 ^{o}C and then incubated at 37 ^{o}C for one hour. Finally, the cell suspensions were plated on an appropriate antibiotic-containing LB plates which were incubated at 37 ^{o}C for 16 h.

2.5.5. Sequence verification

Eight colonies were selected from each ligation and plasmid DNA isolated for characterization by restriction digestion. One plasmid with the correct restriction pattern was subsequently transformed into JM109 because better quality DNA for sequencing was obtained from this strain than from NM522. Plasmids isolated from JM109 were then subjected to DNA sequencing to confirm that no mistakes had been introduced during PCR replication.

Approximately, 300 ng of DNA was added to a final sequencing reaction volume of 20 µL containing 1.4 pM of T3 or T7 primer, 0.5 µL of Big Dye® Terminator v1.1 Cycle Sequencing Kit (Applied Biosystems). The reaction mixture was then subjected to 25 cycles of PCR using a TC512 thermal cycler (Techne) with denaturation, annealing and extension steps of 10 sec at 96 ^{o}C (5 min for first round), 5 sec at 50 ^{o}C and 4 min at 60 ^{o}C, respectively. After the addition of 2 µL of 125 mM EDTA, 2 µL of 3 M sodium acetate and 60 µL of 95% ethanol, followed by 15 minute at room temperature, the DNA

was pelleted by centrifugation for 15 minutes, washed with 60 µL of 70% ethanol and dried in a desiccator. The DNA was then dissolved in 20 µL of Hi-Dye Formamide (Applied Biosystems) and denatured at 96 ^{o}C for 5 min. Finally samples were loaded onto a 96-well sequencer tray and sequenced using a 3130 Genetic Analyzer (Applied Biosystems). The sequence was verified manually.

2.5.6. Cloning in pET vector

After sequence verification, the gene was removed from the pKS- vector with appropriate restriction enzymes and ligated into pET28b which was cut with the same enzymes following the procedure described above. Plasmid DNA from transformed colonies of *E. coli* BL21 was screened to identify one with the expected size and restriction pattern. An aliquot of the culture was stored in 24 % DMSO at -60 ^{o}C.

Table 2-3: Protein expression plasmids used over the course of the study

Plasmid	**Cloning restriction sites**	**Purification tag**
pET28b− *pex6*	Sal1/Not1	6X His-tag
pET28b – *pex18*	Sst1/Xho1	6X His-tag (N- and C- terminal)
pET28b – *pex21*	HindIII/BamHI	6X His-tag (N- and C-terminal)
pET28b – *idp3*	BamHI/HindIII	6X His-tag

2.6.1 Recombinant protein expression

Small scale (30 mL) cultures of transformed and untransformed strains were grown at 37 ^{o}C in LB medium to OD_{600} ~ 0.6 at which time IPTG at either high (1 mM) or low (0.1 mM) concentration was added to induce RNA and protein synthesis. As part of the screening process to identify optimum conditions, the induced cultures were then grown at room temperature, 28 ^{o}C, and 37 ^{o}C for 4 to 16 hours. The inductions of PEX6, PEX21 and IDP3 were best with 0.1 mM IPTG whereas the induction of PEX18 was best at 1 mM IPTG. The optimum temperature in all cases was 28 ^{o}C. Large scale induction was then carried out in 500 mL cultures using these conditions.

2.6.2 Recombinant protein purification

Large scale cultures were centrifuged at 7000 rpm for 10 min and the cell pellets frozen at -60 ^{o}C. After thawing, cells were suspended in a ratio of 75 g of cells per 400 mL of lysis buffer (50 mM potassium phosphate (KPi) pH 7.0, 1 mM EDTA) with gentle stirring at 4 ^{o}C for 30 min. The suspension was then passed through a French Press at 20,000 psi three times and the cell debris was removed by centrifugation. The supernatant was then used for protein purification with the specific steps varying slightly among the different proteins. For all but IDP3, the purification was initiated by the addition of streptomycin sulfate to a final concentration of 2.5% and stirring for 30 min at 4 ^{o}C followed by removal of the precipitate by centrifugation. To the clear supernatant, solid ammonium sulfate was added in steps to bring the final salt concentration to 20%, 30%, 40%, 50%, 60% and 70% of saturation. The solution was stirred for 30 minutes with each successive addition followed by centrifugation to remove precipitated protein. The protein pellets at each step were resuspended in 50 mM KPi pH 7.0 or in 50 mM Tris-

HCl pH 8.0 and analyzed for protein content by SDS polyacrylamide gel electrophoresis. Fractions with the desired protein were pooled and dialyzed twice against 2 L of 50 mM KPi pH 7.0 or 50 mM Tris-HCl pH 8.0 as needed.

2.6.2.1. Purification of IDP3

After cell lysis by French press and clarification by centrifugation, the supernatant was passed through a column of glass wool to remove any floating debri. Eluate containing about 160 mg of protein was injected onto a Ni-NTA column and then washed with 8-10 column volumes of binding buffer. After washing with binding buffer and also with 25 mM imidazole in the same buffer, the protein was eventually eluted with 100 mM and 200 mM imidazole and ran on SDS gel to check for its presence. After confirming the presence of pure IDP3 in the fractions by SDS-PAGE, the selected fractions were pooled and concentrated by Amicon concentrator (model 8050) using an YM-30 membrane to a final concentration of 12 mg/mL. The final purified IDP3 was dialyzed further against 2 litres of 50 mM Tris-HCl, pH 8.0 and stored at -60 ^{o}C until needed.

2.6.2.2. Purification of PEX18

Initial attempts to purify PEX18 involved both affinity chromatography on nickel columns and ion exchange chromatography on DEAE cellulose. To enhance protein affinity for the nickel resin, the protein was first denatured to expose the His-tag which seemed to be buried in the protein. This was achieved by first lysing the cells using a suspension solution of 50 mM Tris, pH 8.0, 0.1 M NaCl, 10% glycerol and 4 M urea and three passages through the French press as described above. After clarification, about 160 mg of protein was loaded on a nickel-nitrilotriacetic acid (Ni-NTA) Superflow resin

(Qiagen) in a XK-16 column (Amersham Biosciences Inc., Canada). NTA has four chelation sites for nickel ions which help in much more tighter binding than IDA; the later has three sites available for interaction with nickel. The extra chelation site prevents nickel-ion leaching and results in greater binding capacity. The column was then washed sequentially with 8 column volumes of binding buffer followed by 10 column volumes each of 50 mM, 100 mM and 200 mM imidazole in the binding buffer. The selected fractions were pooled after confirming its presence with the help of SDS-PAGE and dialyzed overnight at 4 ^{o}C against a renaturing buffer containing 0.5 M KCl, 10 mM sodium citrate, pH 6.8, 1 mM DTT and 10% glycerol. An aliquot of the final purified PEX18 was loaded on Ni-NTA resin to check whether it binds to the column or not. PEX18 does not bind to the column and comes out in flow through suggesting that the protein has successfully renatured back to its native state. It was then concentrated under nitrogen in a stirred pressure cell (Amicon, model 8050) using an YM-10 membrane to a final concentration of 12-15 mg/mL. The final purified PEX18 was dialyzed further against 2 litres of 50 mM Tris-HCl, pH 8.0 and stored at -60 ^{o}C until needed.

2.6.2.3. Purification of PEX21

Like PEX18 neither affinity nor ion exchange chromatography provided pure protein and the denaturation protocol was employed. Ultimately, a protocol identical to that outlined for PEX18 was successfully applied to PEX21.

2.6.2.4. Purification of PEX6

The purification of PEX6 from the crude extract was not at all straight forward and several protocols were investigated. The first protocol involved affinity chromatography on a 1 mL HiTrap nickel column (GE Health Sciences Inc., Canada).

Immobilized Metal-ion Affinity Chromatography (IMAC):

This protein purification technique is based on the interaction of histidine, cysteine and tryptophan side-chains with the transition metal ions such as Cu^{2+}, Ni^{2+}, Co^{2+}, Zn^{2+} which are immobilized via iminodiacetic acid (IDA) to a porous chromatographic support (Belew and Porath, 1990). These columns are packed with highly cross-linked agarose beads to which IDA has been coupled by stable ether groups via a spacer arm of seven atoms. Nickel has a higher affinity for imidazole rather than histidine, even though both share the same functional group (imidazol ring). Hence, the elution of the purified his-tagged proteins can be achieved by increasing the imidazole concentration in the buffer. The resin was first charged with 0.1 M $NiSO_4$, washed with water and then with binding buffer containing 50 mM KPi pH 8.0 and 0.5 M NaCl. The protein mixture containing the His-tagged PEX6 was loaded on the column, eluted with a step up gradient of imidazole concentration like 25 mM, 50 mM and checked by SDS-PAGE. Other combinations of imidazole, of NaCl concentrations and even replacing the nickel with cobalt were investigated.

Size exclusion chromatography was also attempted using Superose 12. The column (particle size 11 µm, optimal separation range M_r 1kD–300kD) was equilibrated with 50 mM Tris-HCl pH 8.0, 150 mM NaCl, after which 5 mg of protein from the ammonium sulfate fractionation, dialyzed into the same buffer, was loaded and eluted. A constant flow of 0.2 mL/min was applied using a FPLC apparatus (BIORAD) and 0.5 mL fractions were collected. An aliquot of each sample was analyzed by SDS PAGE. Samples with the desired protein were pooled and concentrated (YM 30 filter in an Amicon concentrator). Subsequent purification on a nickel column was attempted. In

addition, a Superdex 200 column (separation range 10kD-600kD, GE Health Sciences) was investigated using the same buffers.

Finally ion exchange chromatography on cellufine A-500 resin (Chisso America) was investigated.

Ion Exchange Chromatography (IEC):

This is a useful purification technique which is based on the reversible interaction between a charged molecule in solution and an oppositely charged group on the matrix. This was initially used to purify basic proteins (Hirs et al., 1951) but later, it was used to separate wide range of proteins due to the introduction of cellulose-based matrices, e.g., carboxymethyl (CM) and diethylamnoethyl (DEAE) (Sober and Peterson, 1956). DEAE is a positively charged weak anion exchanger with a working pH range 3-8 and is used to purify both proteins and nucleic acids. Therefore, the resin can bind negatively charged proteins which can be released by increasing the salt concentration. A 2.5 x 24 cm column bed was poured, washed with 150 mL of 50 mM Tris-HCl pH 7.0 and then charged with protein from the ammonium sulfate fractionation. The column was washed with 50 mM of Tris-HCl pH 7.0 until the A_{280} reached 0.05 after which a linear gradient of 500 mL of 50 mM Tris-HCl, pH 8.0 and 500 mL of 0.5 M NaCl in the same buffer was applied and 80 drop fractions were collected. The fractions containing PEX6 were pooled and concentrated with the help of Amicon (model 8050) using an YM-30 membrane to a final concentration of 1 mg/mL. The concentrated sample was dialyzed against 1 litre of 50 mM Tris-HCl pH 8.0 overnight. The final product was checked for purity by SDS-PAGE and stored in -60 ^{o}C.

2.7. Protein analysis

2.7.1. Determination of protein concentration

Protein concentration was determined spectrophotometrically (Sambrook et al., 1989) based on the absorbance at 280 nm using an Ultrospec 3100 (Milton Roy). During protein purification, the Warburg-Christian method was used to estimate protein concentration (Warburg and Christian, 1941, and Layne, 1957).

2.7.2. Sodium dodecyl sulfate-polyacrylamide gel electrophoresis (SDS-PAGE)

Denaturing SDS-PAGE was carried out according to Weber et al. (1972). A discontinuous polyacrylamide gel consisting of 4% stacking gel and 8-10% gel resolving gel were cast in vertical slabs of dimensions 10 x 10 cm and 0.5 mm thickness. The molecular protein benchmark (Benchmark^{TM}) was purchased from Invitrogen Inc., Canada and this was used in all SDS-PAGE analysis of protein fractions for approximate weight determination. Samples loaded onto the gel usually contained 5-10 µg of protein. Samples were mixed with equal volumes of reduced sample buffer (3.4 mg/mL NaH_2PO_4, 10.2 mg/mL, $NaHPO_4$, 10 mg/mL SDS, 0.13 mM 2-mercaptoethanol, 0.36 g/mL urea and 0.15% bromophenol blue) and boiled for 3 minutes before loading. A constant 150 volts was used to run the gels in a running buffer (14 g/L glycine, 3 g/L Tris base, and 1 g/L SDS) until the dye reached the bottom, using a vertical BIO-RAD mini-Protean II electrophoresis system. Gels were stained with a solution containing 0.5 g/L Coomassie Brilliant Blue R-250, 30% ethanol and 10% acetic acid, and destained with repeated changes of destaining solution containing 15% methanol and 7% acetic acid until the background was clear. Another destaining solution containing 7% acetic acid and 1%

glycerol was used to soak the gels before mounting on 3 mm Whatman paper, covered with clear plastic film, and dried at 80 ^{o}C for 1 hour on a slab gel drier under vacuum.

2.8. Enzyme activity

The enzymatic activity of IDP3 was determined by monitoring NADPH production at 340 nm (Ultrospec 3100 pro) in 1ml assays containing 50 mM KPO_4 (pH7.5), 10 mM $MgCl_2$, 0.25 mM $NADP^+$ and 2.5 mM isocitrate at 25 ^{o}C (Loftus et al., 1994). One unit of isocitrate dehydrogenase activity is 1 µmol of NADPH produced per minute.

3. RESULTS

The primary objective of this research is to express and purify a selection of proteins from the yeast peroxisome leading ultimately to a solution of their structures by X-ray crystallography. The specific proteins included in this study are isocitrate dehydrogenase 3 (IDP3), and peroxins 18, 21 and 6 (PEX18, PEX21 and PEX6).

3.1. IDP3

3.1.1. Protein expression

The pET28b-*IDP3* clone was constructed by J. Switala and provided for the work described here. Growth temperature and IPTG concentration were screened to determine that similar expression of IDP3 was obtained with either 0.1 or 1 mM IPTG and either 28 ^{o}C or 37 ^{o}C (Fig. 3-1). IDP3 migrated on SDS-PAGE at ~50 kDa consistent with its predicted size of 48 kDa.

3.1.2. Purification of IDP3

The purification of IDP3 was achieved by affinity chromatography involving Ni-NTA Superflow resin. Initially, a step gradient of 25 mM, 50 mM and 250 mM was used, but ultimately a two step elution protocol with 100 mM and then 200 mM was determined to be most effective (Fig. 3-2, panel A and B). Fractions containing IDP3 were pooled and concentrated to 13.2 mg/mL (Fig. 3-2, panel C).

3.1.3. Enzyme activity

The enzyme activity of IDP3 was determined spectrophotometrically by measuring the increase of NADPH absorbance at 340 nm. A specific activity of 77 µmol/min/µg was determined which compares to 99.2 µmol/min/µg as previously published by Henke et al., 1997.

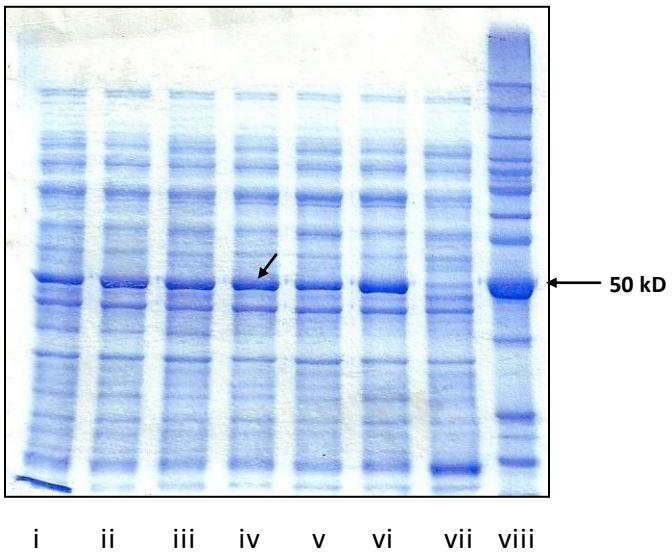

Figure 3-1: Small scale protein expression trials; (A) Protein extracts from cultures of BL21/pET28-IDP3 induced in various ways are shown after separation by SDS-PAGE. Protein samples in lanes i, iii, vii are from cultures induced with 1 mM IPTG at room temperature, 28 ^{o}C and 37 ^{o}C respectively. Protein samples in lanes ii, iv (shown by arrow) and vi are from cultures induced with 0.1 mM IPTG at room temperature, 28 ^{o}C and 37 ^{o}C, respectively. Lane vii contain protein extract from control BL21 cells. Lane viii contains protein size markers.

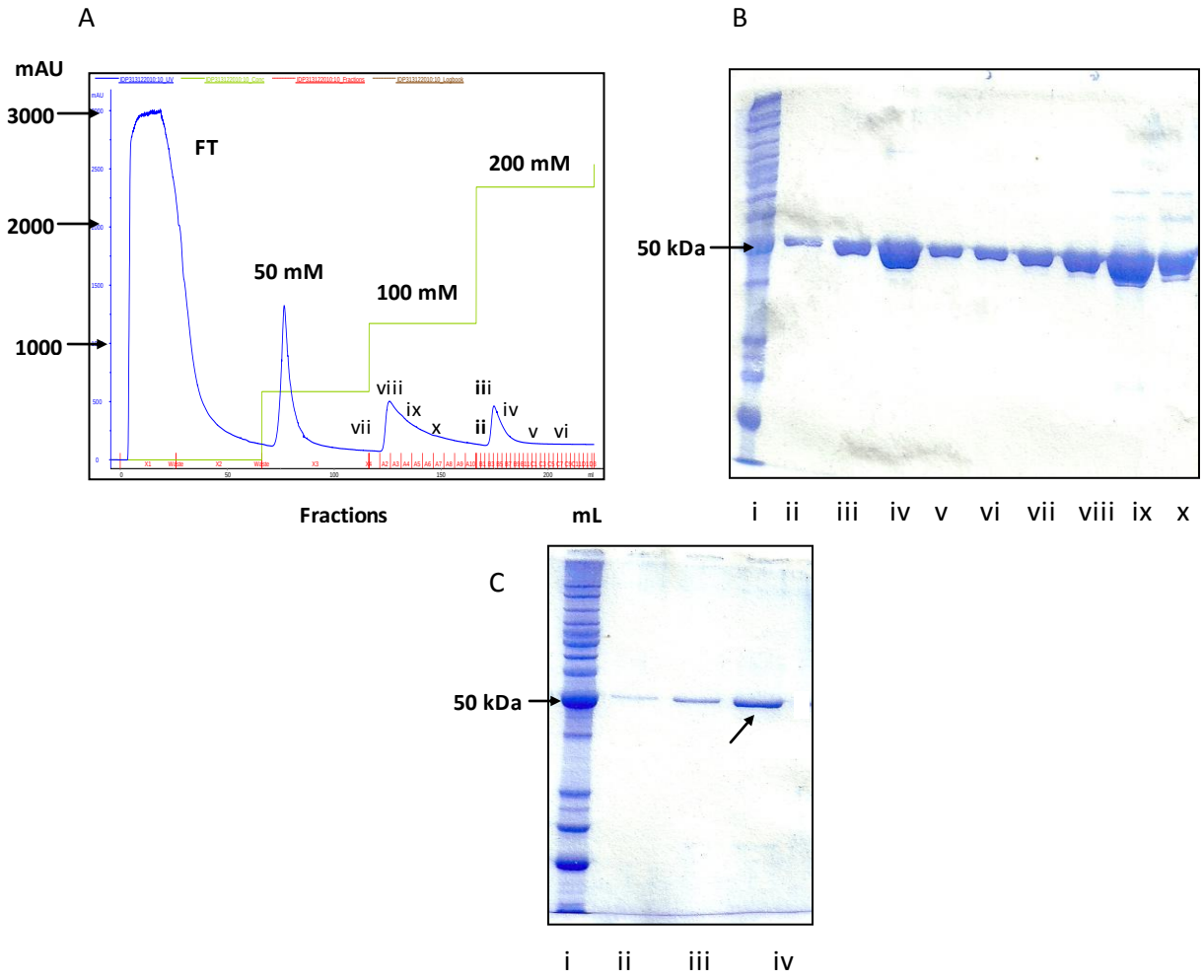

Figure 3-2: Purification of IDP3 using Ni-NTA Superflow resin; (A) Elution profile of protein when passed through Ni-NTA Superflow resin assayed at A_{280} nm. (B) Lanes containing protein fractions at various stages of elution for IDP3 purification which are separated by SDS-PAGE as follows: ii through vi contain the pure IDP3 eluted with 200 mM imidazole; vii through x contain IDP3 eluted with 100 mM imidazole. Lane i contains the protein size markers. (C) Lane ii, iii and iv contain 1 µg, 3 µg and 5µg (shown by arrow) of pure IDP3 respectively. Lane i contains protein size markers.

3.2. PEX18

3.2.1. Construction of PEX18 expression vectors

The approximately 850 bp DNA fragment containing the PEX18 gene was amplified by PCR from a yeast chromosomal clone obtained from Open Biosystems using primers containing *Sst*1 and *Xho*1 restriction sequences (Fig. 3-3, panel A and B). From the pKS-PEX18 clone, the *Sst*I-*Xho*I fragment was cloned into pET28b cut with the same restriction nucleases to generate pET28-PEX18 (Fig. 3-3, panel C). The resulting clone was designed to have His-tags attached at both the N- and C-terminal ends.

3.2.2. Protein expression

Growth temperature and IPTG concentration were screened to determine the optimal conditions for PEX18 as 1 mM IPTG at 28 ^{o}C. The predominant band of expressed protein migrated at approximately 42 kDa somewhat larger than the expected 32 kDa (Fig. 3-4).

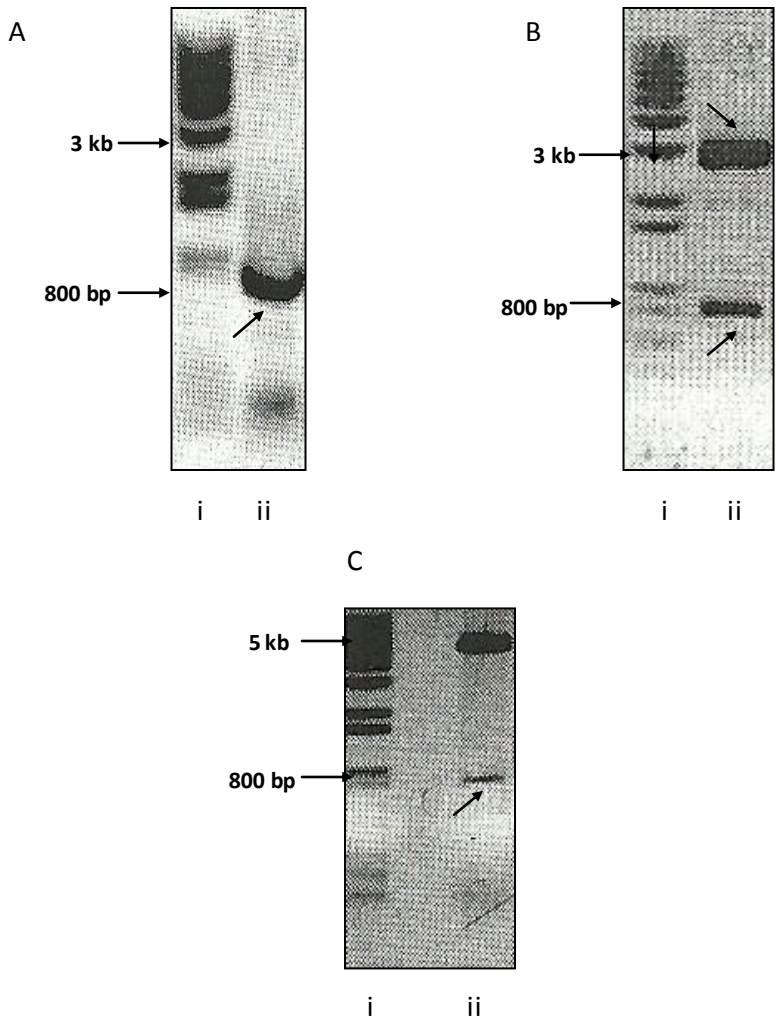

Figure 3-3: Construction of pET28-*PEX18*; (A) Lane ii contains the PCR product of *PEX18* gene (marked by arrow) and lane i contains the 1 kb DNA ladder. (B) Lane ii contains the *Sst*I + *Xho*I restriction digests of DNA from transformant produced in the insertion of the *PEX18*-containing PCR product into pKS-. The pKS- vector migrates at 2.9 kb (marked by upper arrow) and the *PEX18* insert migrates near 800 bp (marked by lower arrow). Lane i contains the DNA ladder. (C) Lane ii contains the *Sst*I + *Xho*I restriction digest mixtures of DNA from a transformant produced in the ligation of the 851 bp fragment into pET28b. The pET28b vector migrates at 5.3 kb and the *PEX18* insert at 851 bp (marked by arrow). Lane i contains the DNA ladder.

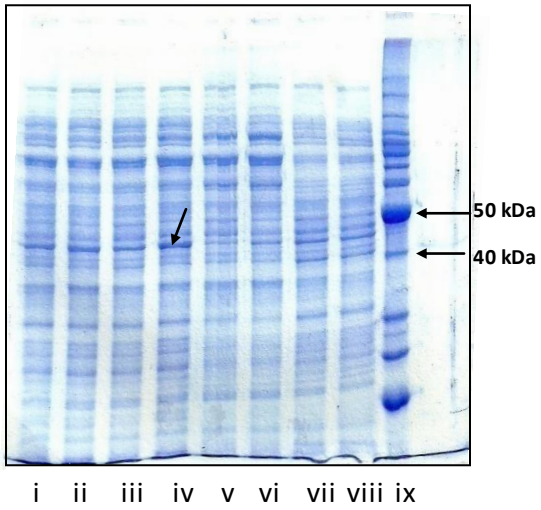

Figure 3-4: Small scale protein expression trials; Protein extracts from cultures of BL21/pET28-PEX18 induced in various ways are shown after separation by SDS-PAGE. Protein samples in lanes i, iii, vii are from cultures induced with 1 mM IPTG at room temperature, 28 °C and 37 °C respectively. Protein samples in lanes ii, iv (shown by arrow) and viii are from cultures induced with 0.1 mM IPTG at room temperature, 28 °C and 37 °C, respectively. Lane v and vi contain protein extract from control BL21 cells and uninduced BL21 cells respectively. Lane ix contains protein size markers.

3.2.3. Purification of PEX18

Several protocols were investigated in an attempt to purify PEX18 and affinity chromatography was the first. Unfortunately, attempts to bind PEX18 onto the nickel resin were unsuccessful despite having histidine tags at both ends and the protein simply washed through the column in the loading buffer (Fig. 3-5). The second protocol investigated involved size exclusion chromatography using Superose 12, but PEX18 was resolved from the protein mix (Fig. 3-6, panel A). Next, ion exchange on SOURCE 15 Q was investigated, but it too proved unsuccessful (Fig. 3-6, panel B and C).

The inability of PEX18 to bind to a nickel resin suggested that the His tags were buried within the folded protein. Therefore, in an attempt to enhance the protein's affinity for the nickel resin, it was first denatured to expose the His-tag (section 2.6.2. in Methods). The protein was loaded on a Ni-NTA column and then washed sequentially with 8 column volumes of binding buffer followed by 10 column volumes each of 50 mM, 100 mM and 200 mM imidazole in the binding buffer (Figure 3-7, panel A). The fractions eluted with 100 mM and 200 mM imidazole were analyzed on SDS PAGE (Figure 3-7, panel B). The protein was successfully renatured as the protein did not bind to the Ni-NTA resin and eluted in the flow through (Figure 3-7, panel C) and concentrated to 12-15 mg/mL (section 2.6.2. in Methods).

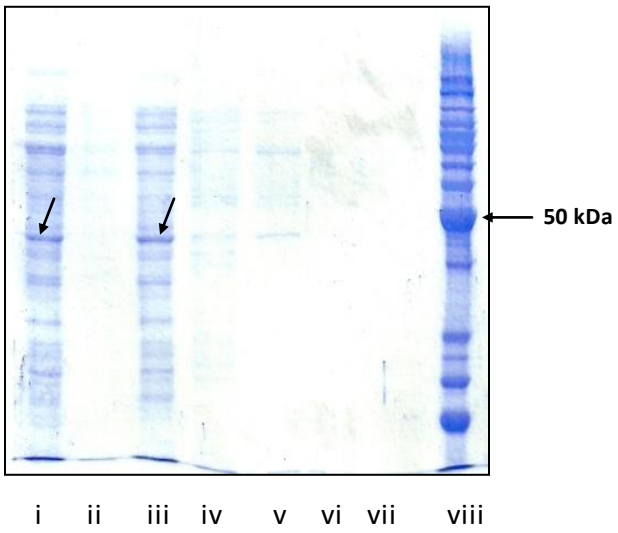

Figure 3-5: Initial purification trials to isolate PEX18 by nickel column; Lanes containing protein fractions from various elution stages which are separated by SDS-PAGE as follows: i and iii – flow through and binding wash (shown by arrows) respectively; iv and v - eluted with 25 mM imidazole; lane vi and vii contains very less amount of protein while eluting with 50 mM imidazole; lane viii contains protein size markers.

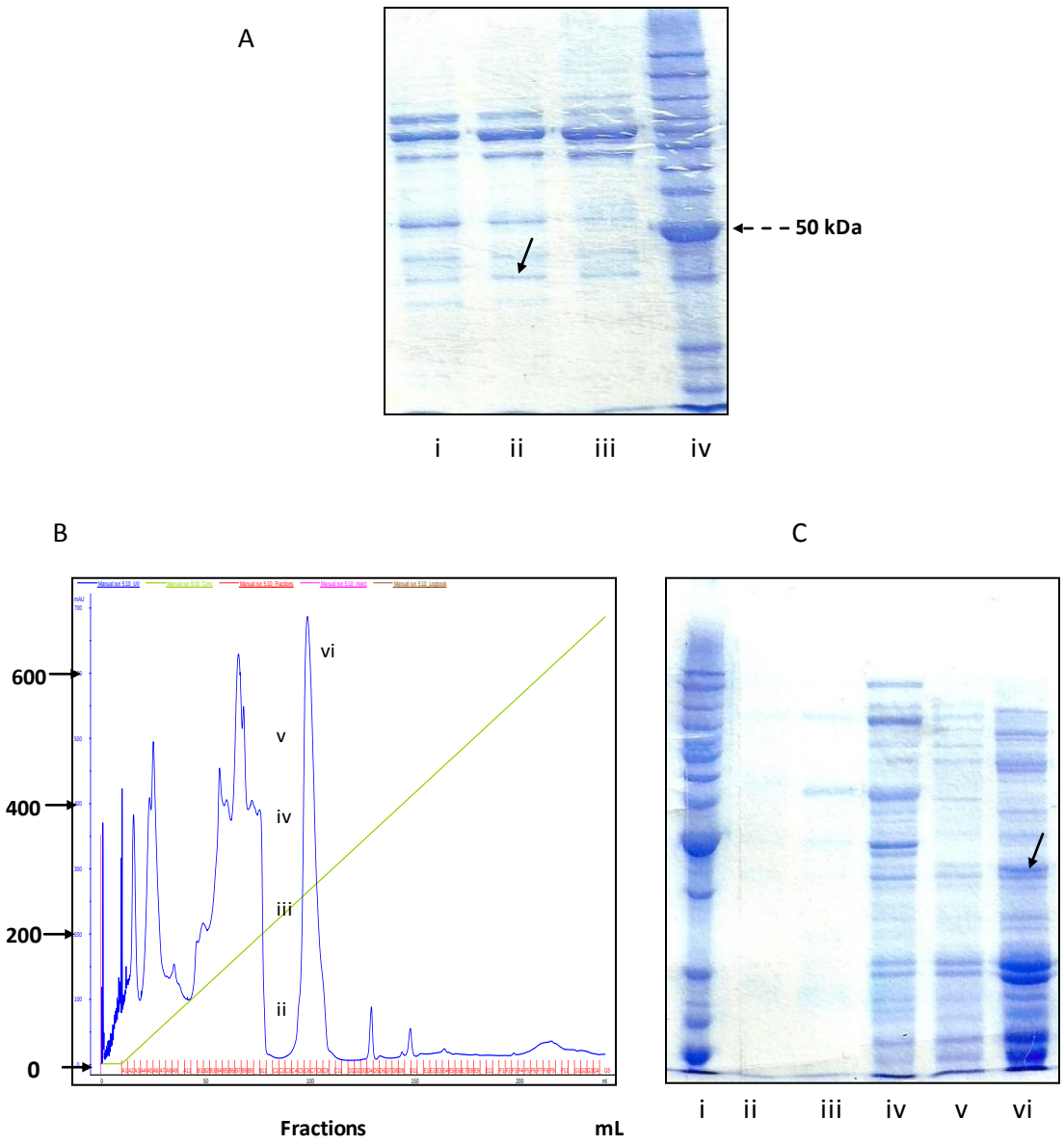

Figure 3-6: Initial purification trials to purify PEX18 by Superose 12 column and SOURCE 15Q strong anionic exchanger column; (A) Lanes i, ii and iii contain the desired protein (shown by arrow) from the various stages of PEX18 purification by Superose 12 column and are separated by SDS-PAGE. Lane iv contains protein size markers. (B) Elution profile of protein assayed at A_{280} nm when the crude extract was passed through SOURCE 15Q anionic exchanger. The various colours in the elution profile are depicted as follows: green = linear increase in salt concentration, blue = protein peaks, red = fractions collected in mL, pink = protein inject point. (C) Lanes ii through vi (shown by arrow) contain PEX18 with other contaminant proteins. Lane i contains the protein size markers.

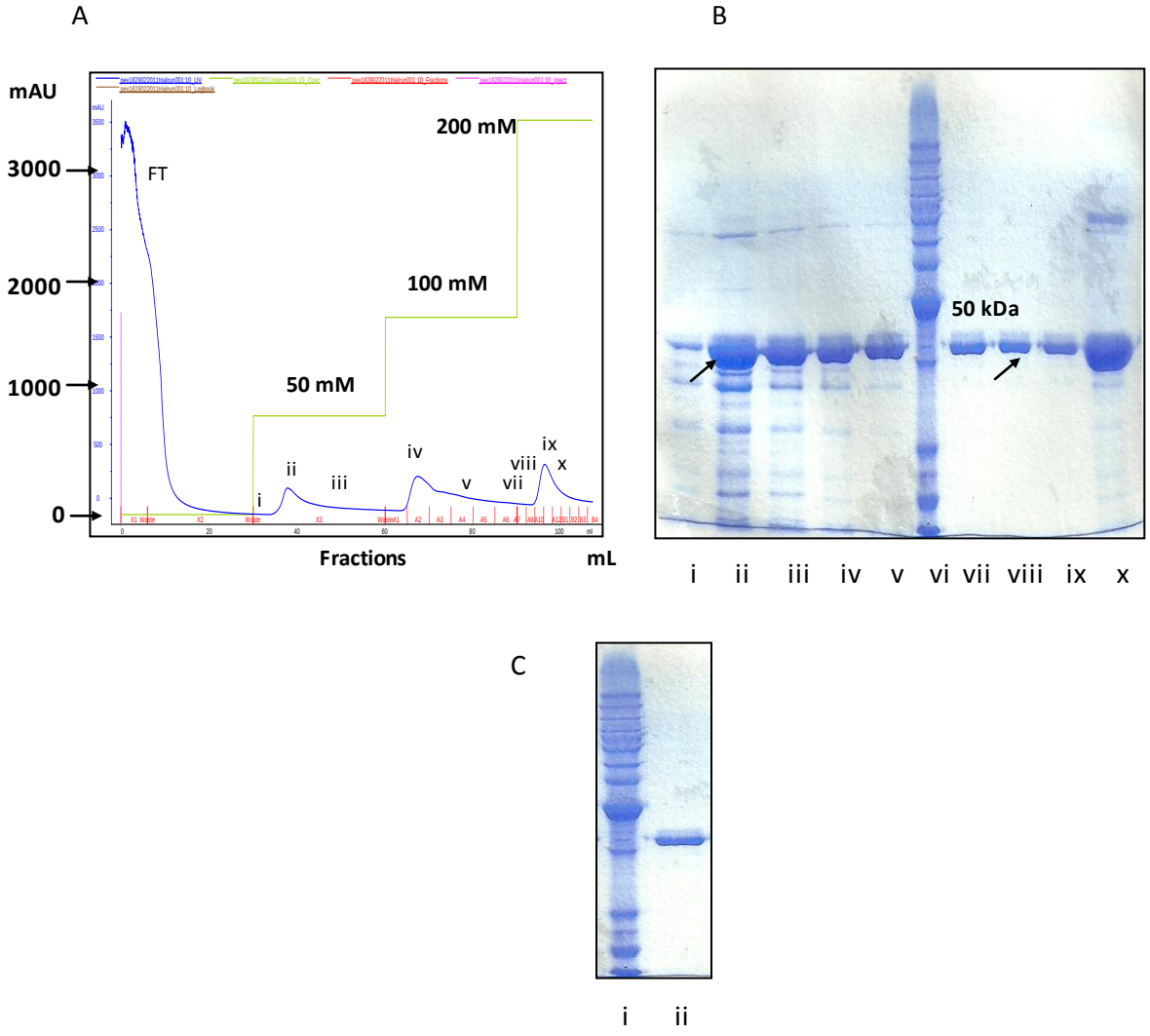

Figure 3-7: Purification of PEX18 under denaturing condition; (A) Elution profile of protein assayed at A_{280} nm when passed through Ni NTA Superflow resin. (B) Lanes containing protein fractions at various stages of elution for PEX18 purification which are separated by SDS-PAGE as follows: i, ii (shown by arrow), iii – protein fractions eluted with 50 mM imidazole; iv and v – fractions eluted with 100 mM imidazole, vii, viii (shown by arrow), ix and x - protein fractions eluted with 200 mM imidazole; Lane vi contains the protein size markers. (C) Lane ii contains the purified PEX18 in the flow through and which did not bind to the resin; lane i contains the protein size markers.

3.3. PEX21

3.3.1. Construction of PEX21 expression vectors

The approximately 866 bp DNA fragment containing the *PEX21* gene was amplified by PCR from a yeast chromosomal clone obtained from Open Biosystems using primers containing *Bam*H1 and *Hin*dIII restriction sequences (Fig. 3-8, panel A) and cloned into pKS- which was then used to transform *E.coli* NM522 strain for the purpose of sequence verification (Figure 3-8, panel B). From the pKS-PEX21 clone, the *Bam*HI-*Hin*dIII fragment was transferred into pET28b cut with the same restriction endo-nucleases to generate pET28-PEX21 (Fig. 3-8, panel C).

3.3.2. Protein expression and purification

Growth temperature and IPTG concentration were screened to determine the optimal conditions for PEX21 as 0.1 mM IPTG at 28 ^{o}C (Fig. 3-9). The protein at approximately 33 kDa was precipitated by ammonium sulfate at 70% and 80% of saturation (Fig. 3-10).

Several different protocols were investigated during attempts to purify PEX21. The first was affinity chromatography on 1 mL HiTrap nickel column. While initially appearing promising (Fig. 3-11, panel A), yields were low and the column proved to be unreliable, producing inconsistent results (Fig 3-11, panel B). Size exclusion chromatography proved to be even less successful with very little purification being achieved (Fig. 3-12, panel A and B). Similarly, ion exchange chromatography on SOURCE Q15 did not improve purity significantly (Fig.3-12, panel C and D).

In the end, the denaturation protocol as applied to PEX18 was also successfully applied to PEX21. Denatured protein successfully bound and eluted from nickel-NTA

resin (Fig. 3-13, panel A and B). Modification of the elution conditions eventually yielded pure PEX21 (Fig. 3-13, panel C). The resulting protein was passed through Ni-NTA column and it was found that it did not bind to the resin (Fig. 3-13, panel D) suggesting that it successfully renatured back to its native state and ultimately concentrated to 10 mg/mL.

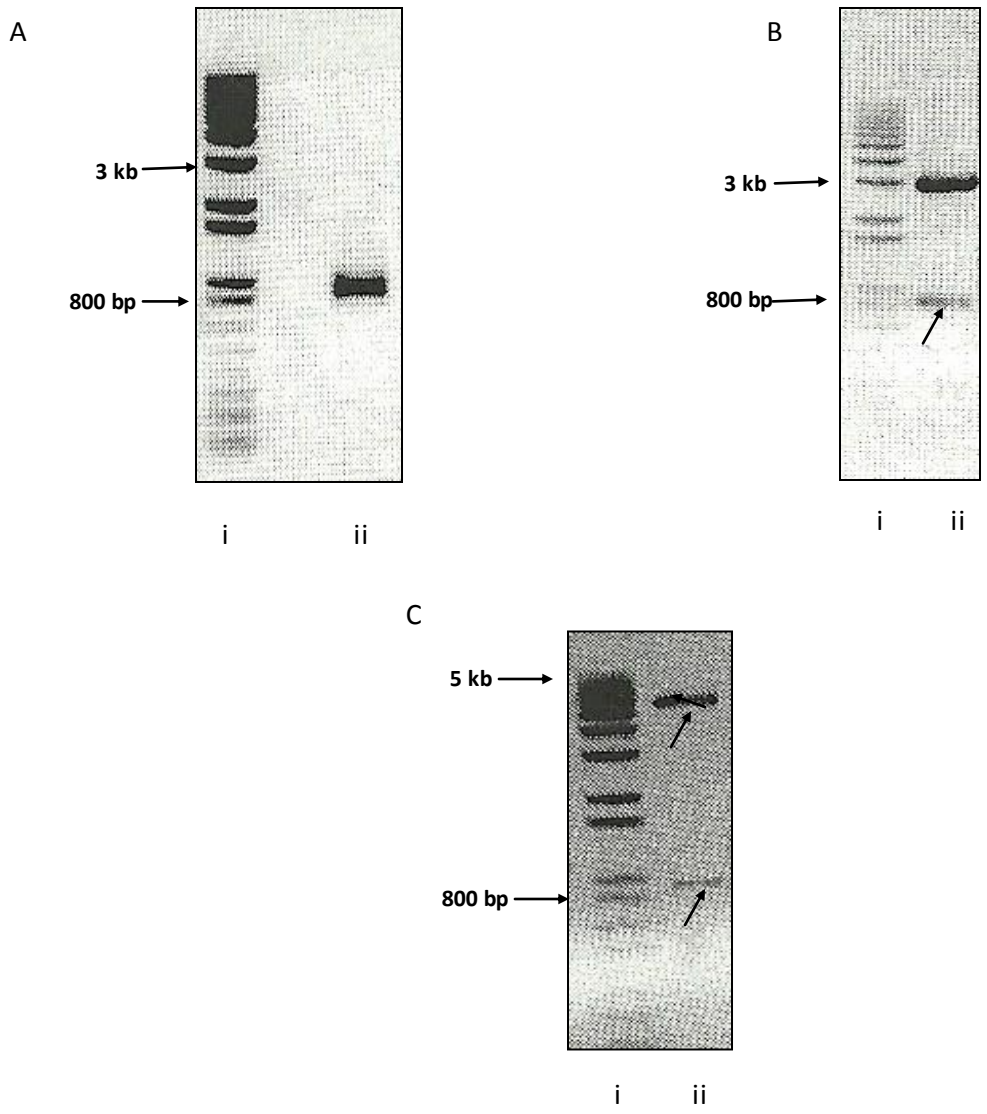

Figure 3-8: Construction of pET28-*PEX21*; (A) Lane ii contains the PCR product of *PEX21* gene and lane i contains the 1 kb DNA ladder. (B) Lane iv contains the *Bam*HI + *Hin*dIII restriction digests of DNA from transformant produced in the insertion of the *PEX21*-containing PCR product into pKS-. The pKS- vector migrates at 2.9 kb and the *PEX21* insert migrates at 860 bp (marked by arrow). Lane i contains the DNA ladder. (C) Lanes ii contains the *Bam*HI + *Hin*dIII restriction digest mixtures of DNA from a transformant produced in the ligation of the 860 bp fragment into pET28b. The pET28b vector migrates at 5.3 kb (marked by upper arrow) and the *PEX21* insert at 860 bp (marked by lower arrow). Lane i contains the DNA ladder.

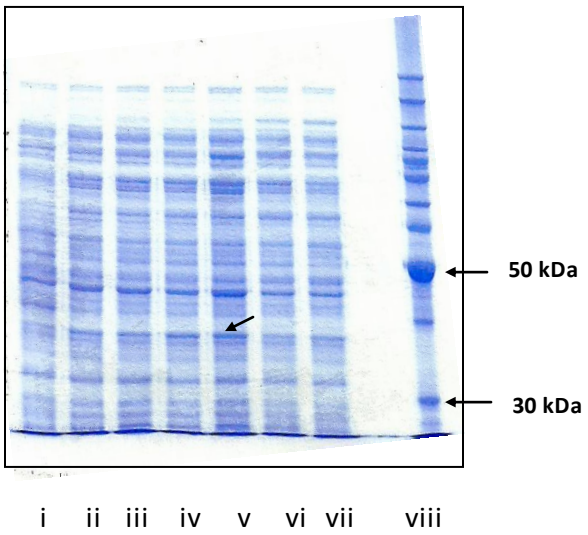

Figure 3-9: Small scale protein expression trials; Protein extracts from cultures of BL21/pET28-*PEX21* induced in various ways are shown after separation by SDS-PAGE. Protein samples in lanes ii, iv, vi are from cultures induced with 1 mM IPTG at room 37 ^{o}C, 28 ^{o}C and room temperature, respectively. Protein samples in lanes iii, v (shown by arrow) and vii are from cultures induced with 0.1 mM IPTG at 37 ^{o}C, 28 ^{o}C and room temperature, respectively. Lane i contain protein extract from control BL21 cells and lane viii contains protein size markers.

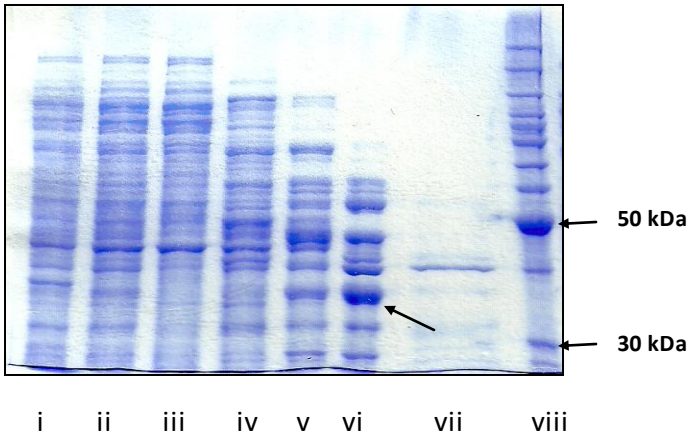

Figure 3-10: Ammonium sulfate fractionation to precipitate PEX21; Lanes i - vii contain protein fractions from the various stages of PEX21 purification are separated by SDS-PAGE as follows: i - crude extract; ii - streptomycin sulfate supernatant; iii, iv, v, and vi - 50%, 60%, 70%, and 80% ammonium sulfate pellets (shown by arrow); vii - 80% ammonium sulfate supernatant. Lane viii contains protein size markers.

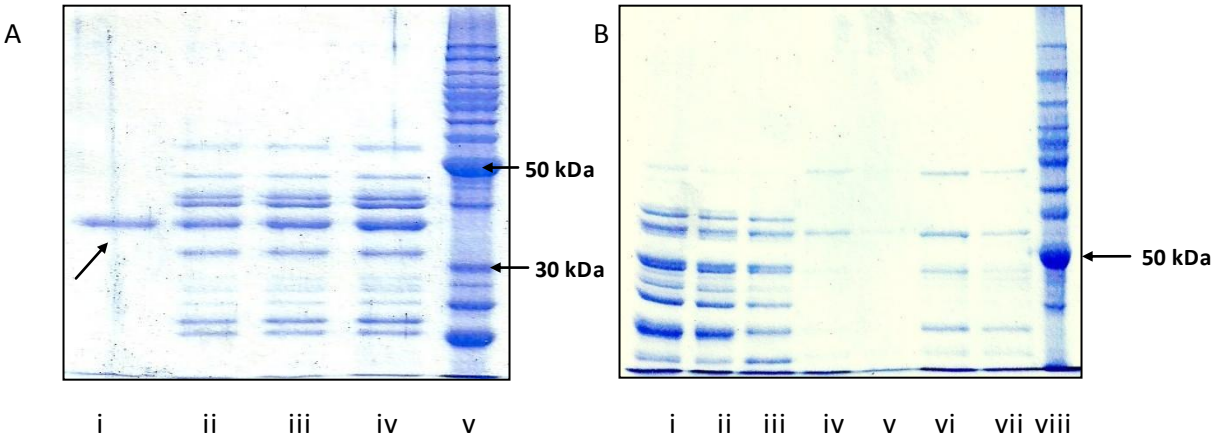

Figure 3-11: Initial purification trials to isolate PEX21 by nickel column; (A) Lanes containing protein fractions from various elution stages which are separated by SDS-PAGE as follows: i – protein fraction eluted with 25 mM imidazole (marked by arrow); ii, iii and iv contain binding wash, flow through and 80% ammonium sulfate fraction respectively; Lane v contains the protein size markers. (B) Lanes containing protein fractions from various elution stages which are separated by SDS-PAGE as follows: i – flow through; ii, iii - binding wash; iv through vii - protein fraction eluted with 25 mM imidazole. Lane viii contains the protein size markers.

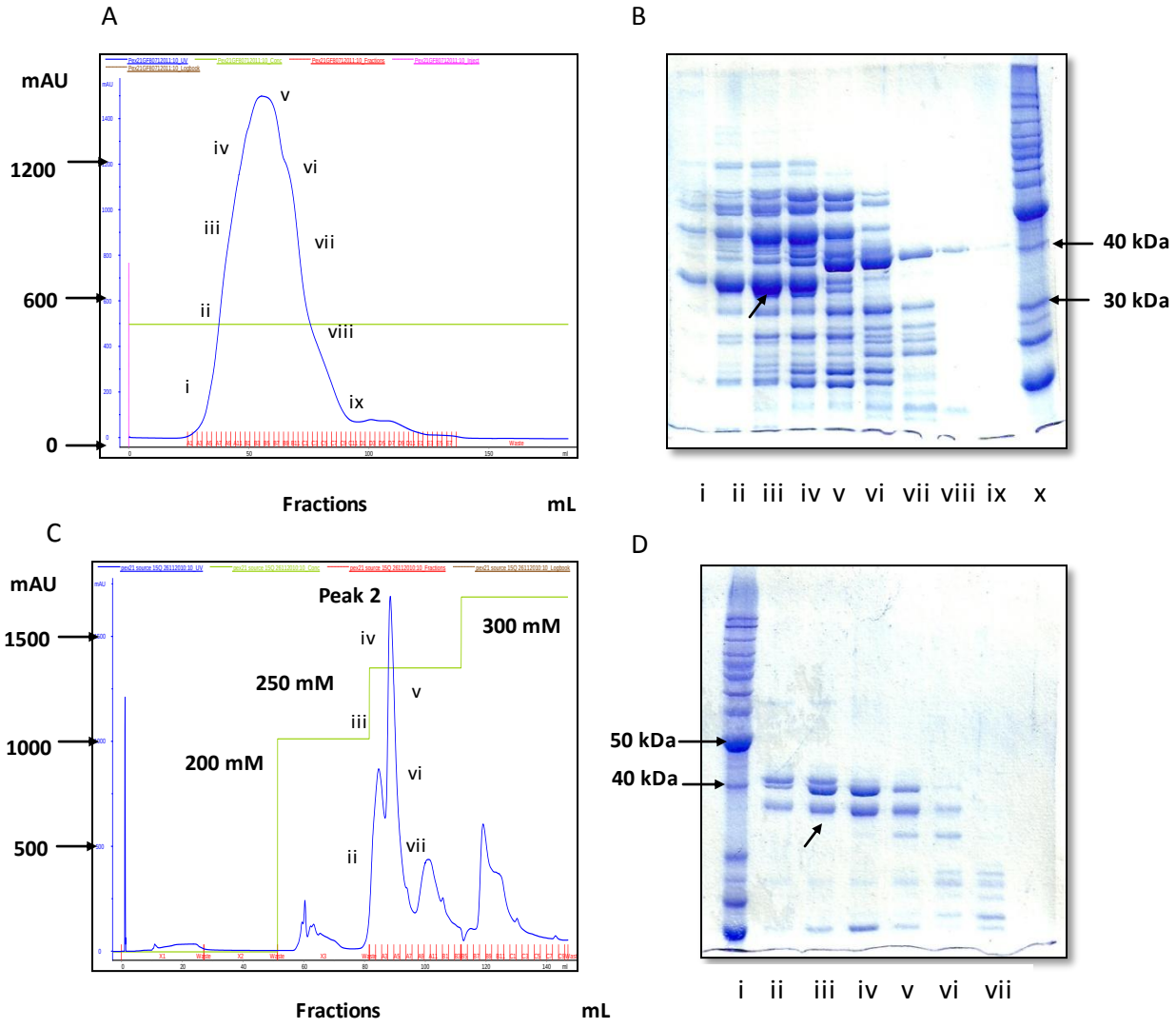

Figure 3-12: Initial purification trials for PEX21; (A) Elution profile of protein assayed at A_{280} nm when passed through Superdex 75 column. (B) Lanes containing protein fractions from various elution stages by Superdex 75 column which are separated by SDS-PAGE as follows: i, ii, iii and iv contain the PEX21 along with other background proteins. Lanes v through ix contain the background proteins. Lane x contains the protein size markers. (B) Elution profile of protein assayed at A_{280} nm when passed through SOURCE 15Q column. (C) Lanes containing protein fractions (peak 2) from various elution stages from SOURCE 15Q column which are separated by SDS-PAGE as follows: ii, iii (shown by arrow), iv and v contain the desired protein fraction; Lane i contains the protein size markers.

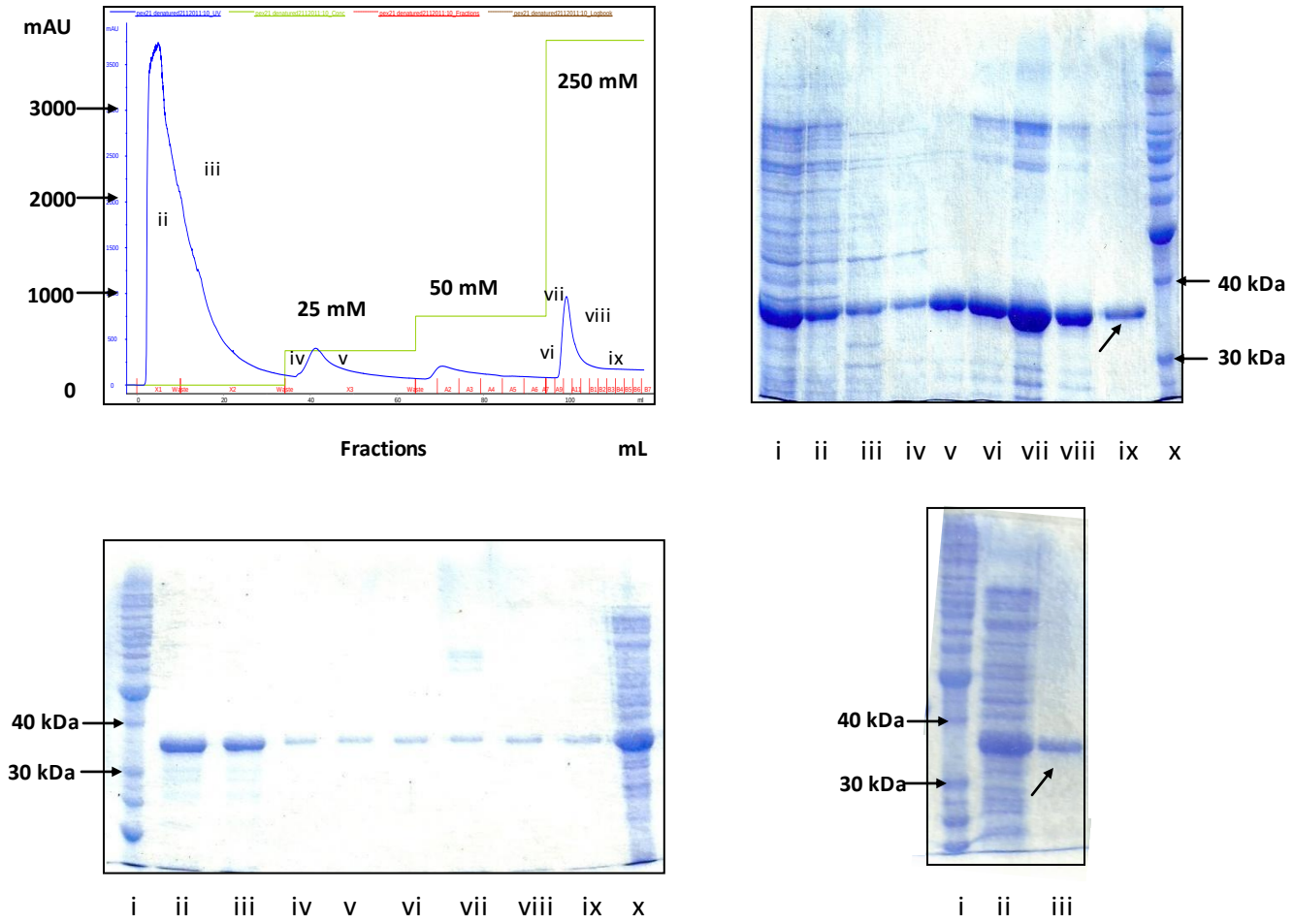

Figure 3-13: Purification of PEX21 under denaturing condition; (A) Elution profile of protein assayed at A_{280} nm when passed through Ni-NTA Superflow resin. (B) Lanes containing protein fractions at various stages of elution for PEX21 purification which are separated by SDS-PAGE as follows: i, ii and iii contain control, flow through and binding wash; iv and v – protein fractions eluted with 25 mM imidazole; vi through ix contain protein fractions eluted with 250 mM imidazole where the pure PEX21 is shown by arrow; lane x contains the protein size markers.(C) Lane ii and iii contains protein fractions eluted from 200 mM imidazole; lane iv through ix contain PEX21 eluted with 100 mM imidazole. Lane i and x contain protein size markers and control sample respectively. (D) Lane ii contains the control sample, unpurified. Lane iii contains the purified PEX21 (shown by arrow) which did not bind to the resin; lane i contains the protein size markers.

3.4. PEX6

3.4.1. Construction of the pET28b-PEX6

After PCR amplification of the DNA fragment containing *PEX6* from a yeast chromosomal clone obtained from Open Biosystems using primers containing *Sal*1 and *Not*1 restriction sequences (Fig. 3-14, panel A), it was cloned into pKS- (Figure 3-14, panel B). After sequence confirmation, the *PEX6*-containing fragment was excised and ligated into pET28b to form pET28-PEX6 (Figure 3-14, panel C) followed by transformation into *E.coli* strain BL21.

3.4.2. Protein expression

After screening both high (1 mM) and low (0.1 mM) IPTG at 22 ^{o}C, 28 ^{o}C and 37 ^{o}C, the best expression of PEX6 was realized with 0.1 mM IPTG at 28 ^{o}C (Fig. 3-15, panel A). Unfortunately, the levels of expression remained low despite these attempts at optimization. For example, several concentrations of glycerol (0.5 to 5%) were added to the growth medium and the *E. coli* Rosetta strain was used to avoid codon bias, without success (Fig. 3-15, panel B).

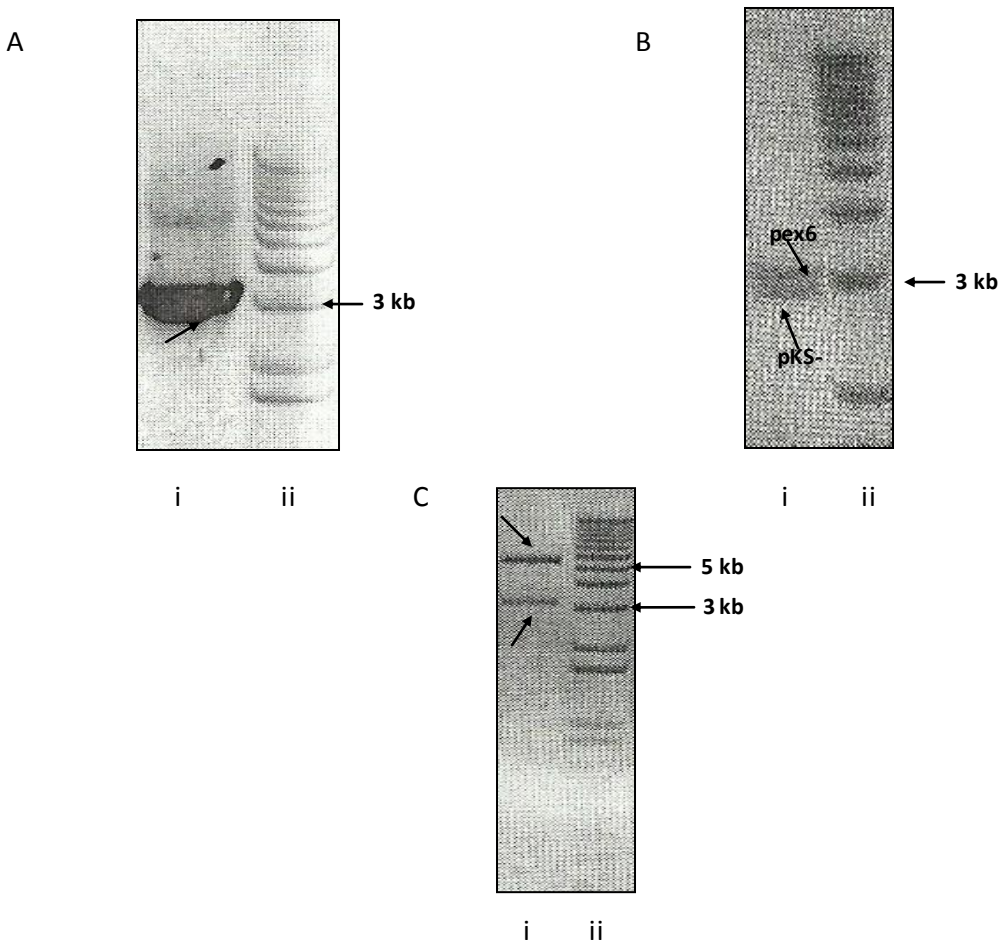

Figure 3-14: Construction of pET28-*PEX6*; (A) Lane i contains the PCR product of *PEX6* gene (marked by arrow) and lane ii contains the 1 kb DNA ladder. (B) Lane i contains the *Sal*I + *Not*I restriction digests of DNA from transformant produced in the insertion of the *PEX6*-containing PCR product into pKS-. The pKS- vector migrates at 2.9 kb (marked by lower arrow) and the *PEX6* insert migrates at 3.1 kb (marked by upper arrow). Lane ii contains the DNA ladder. (C) Lanes i contains the *Sal*I + *Not*I restriction digest mixtures of DNA from a transformant produced in the ligation of the 3.1 kb fragment into pET28b. The pET28b vector migrates at 5.3 kb (marked by upper arrow) and the *pex6* insert at 3.1 kb (marked by lower arrow). Lane ii contains the DNA ladder.

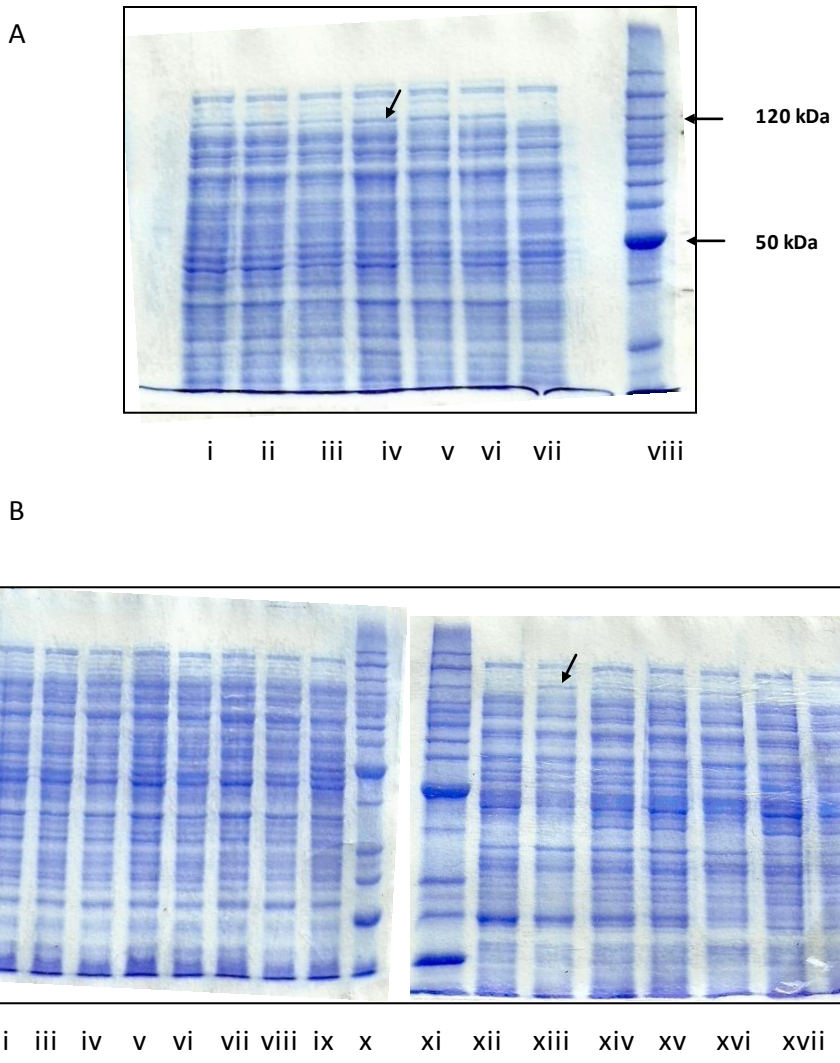

Figure 3-15: Small scale protein expression trials; (A) Protein extracts from cultures of BL21/pET28-PEX6 induced in various ways are shown after separation by SDS-PAGE. Protein samples in lanes i, iii, v are from cultures induced with 1 mM IPTG at room temperature, 28 ^{o}C and 37 ^{o}C respectively. Protein samples in lanes ii, iv and vi are from cultures induced with 0.1 mM IPTG at room temperature, 28 ^{o}C and 37 ^{o}C, respectively. Lane vii contains the protein extract from control BL21 cells. Lane viii contains protein size markers. (B) Protein extract from various trials to enhance the expression. Lanes i through viii represent the increasing concentrations of glycerol from 0.5% to 5% and lane xi represents the culture without glycerol. Lanes xii through xvii represent the small scale expression trials in *E.coli* BL21 Rosetta strain. Lanes xii, xiv and xvi contain high (1mM) induction IPTG at RT, 28 ^{o}C and 37 ^{o}C respectively whereas lanes xiii (position marked by arrow), xv and xvii contain low IPTG (0.1 mM) induction at the above mentioned temperatures respectively. Lane xviii contains the protein loaded from the control BL21 cells. Lane xi contains the protein benchmark.

3.4.3. Purification of PEX6

During the first attempts to purify PEX6, ammonium sulfate precipitation at 30% and 40% saturation was employed (Fig. 3-16, panel A). After resuspension and dialysis, the protein fractions were applied to three different types of column chromatography in attempts to purify it. First, affinity chromatography on a 1 mL HiTrap nickel column was attempted. After washing and elution with imidazole, a protein band at approximately 120 kDa was obtained, consistent with its predicted size of 115 kDa. Unfortunately, several other protein bands were found as contaminants following SDS-PAGE analysis (Fig. 3-16, panel B). Prolonged washing with the loading buffer and loading buffer with low concentrations of imidazole did not improve the purity (Fig. 3-16, panel C). In addition, repeated use of the column gave rise to inconsistent purification resulting in the technique being abandoned.

The second protocol involved size exclusion chromatography which was attempted using Superose 12 and Superdex 200. The ammonium sulfate fractions were loaded on the column and eluted as described in materials and methods. SDS-PAGE analysis of eluted fractions from Superose 12 column revealed that gel filtration did not enhance the purity of PEX6 (Fig. 3-17, panel A and B).

Ion exchange chromatography on DEAE cellulose was also investigated with 600 mg of the 30% and 40% ammonium sulfate fractions being loaded. The fractions were analyzed by absorbance at 280 nm (Figure 3-18, panel A) and were checked by SDS-PAGE and fractions containing PEX6 were pooled and concentrated (Figure 3-18, panels B and C). Unfortunately, the purified protein precipitated upon dialysis and despite investigating several buffer combinations, a protein concentration higher than 1 mg/mL was never achieved.

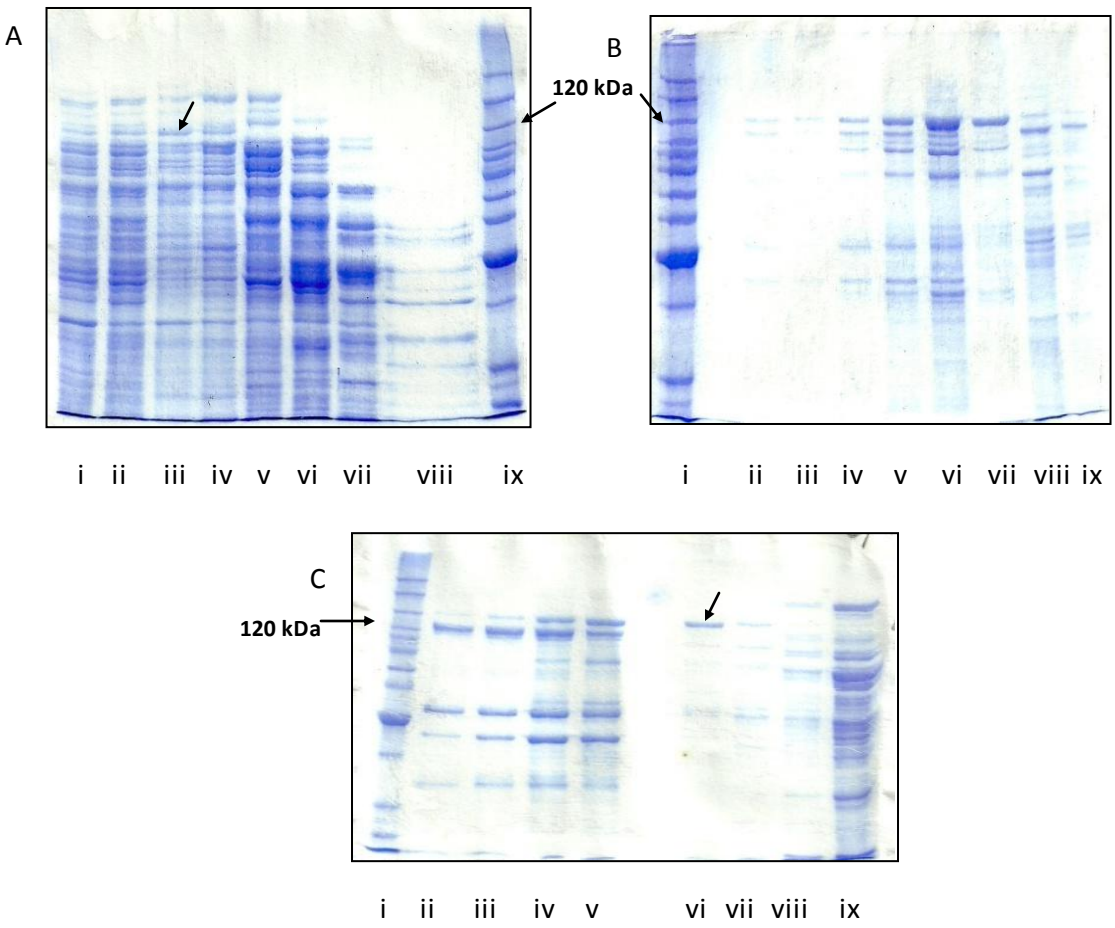

Figure 3-16: Initial purification trials to isolate PEX6 on nickel column; (A) Lanes i - viii contain protein fractions from the various stages of PEX6 purification are separated by SDS-PAGE as follows: i - crude extract; ii - streptomycin sulfate supernatant; iii, iv, v, vi and vii- 30% (shown by arrow), 40%, 50%, 60% and 70% ammonium sulfate pellets; viii - 70% ammonium sulfate supernatant. Lane ix contains protein size markers. (B) Lanes ii and vii contain protein fractions from various elution stages which are separated by SDS-PAGE as follows: ii and iii - eluted with 50 mM imidazole; iv, v, vi,vii - eluted with 25 mM imidazole; lanes viii and ix contain fractions from binding wash and flow through respectively. Lane i contains protein size markers (C) Lanes ii – vii contain protein fractions which were eluted after adding 5 mM or 10 mM in the binding wash and separated by SDS-PAGE. Lanes ii and iii - eluted with 50 mM imidazole; iv and v - eluted with 25 mM imidazole; vi – binding wash containing 10 mM imidazole (shown by arrow), vii – binding wash containing 5 mM imidazole; viii and ix contain binding wash and flow through respectively.

A

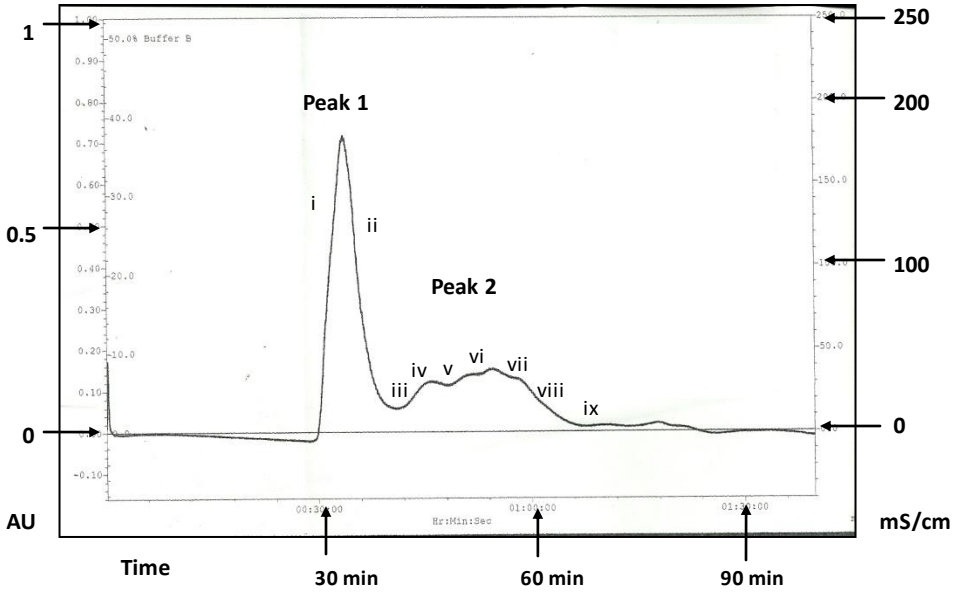

B

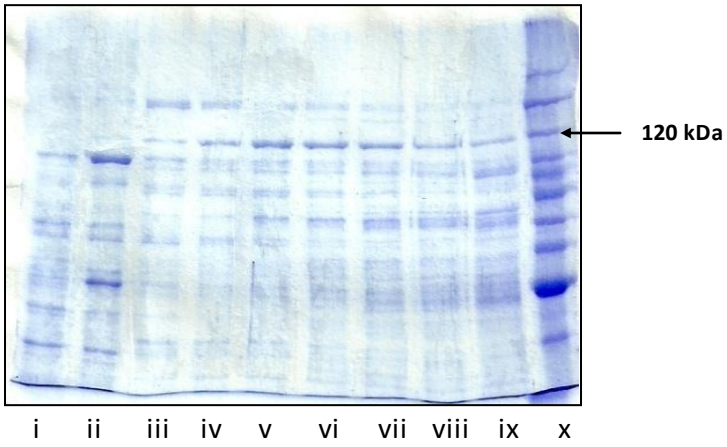

Figure 3-17: Initial purification trials to purify PEX6 on Superose 12 column; (A) Elution profile of protein assayed at A_{280} nm when passed through Superose 12 column. (B) Lanes i - ix contain protein fractions from the various stages of elution from superose 12 column and are separated by SDS-PAGE as follows: Lane i and ii – contains the fractions from peak 1; iii, iv, v, vi, vii, viii and ix – contains the fractions from peak 2.

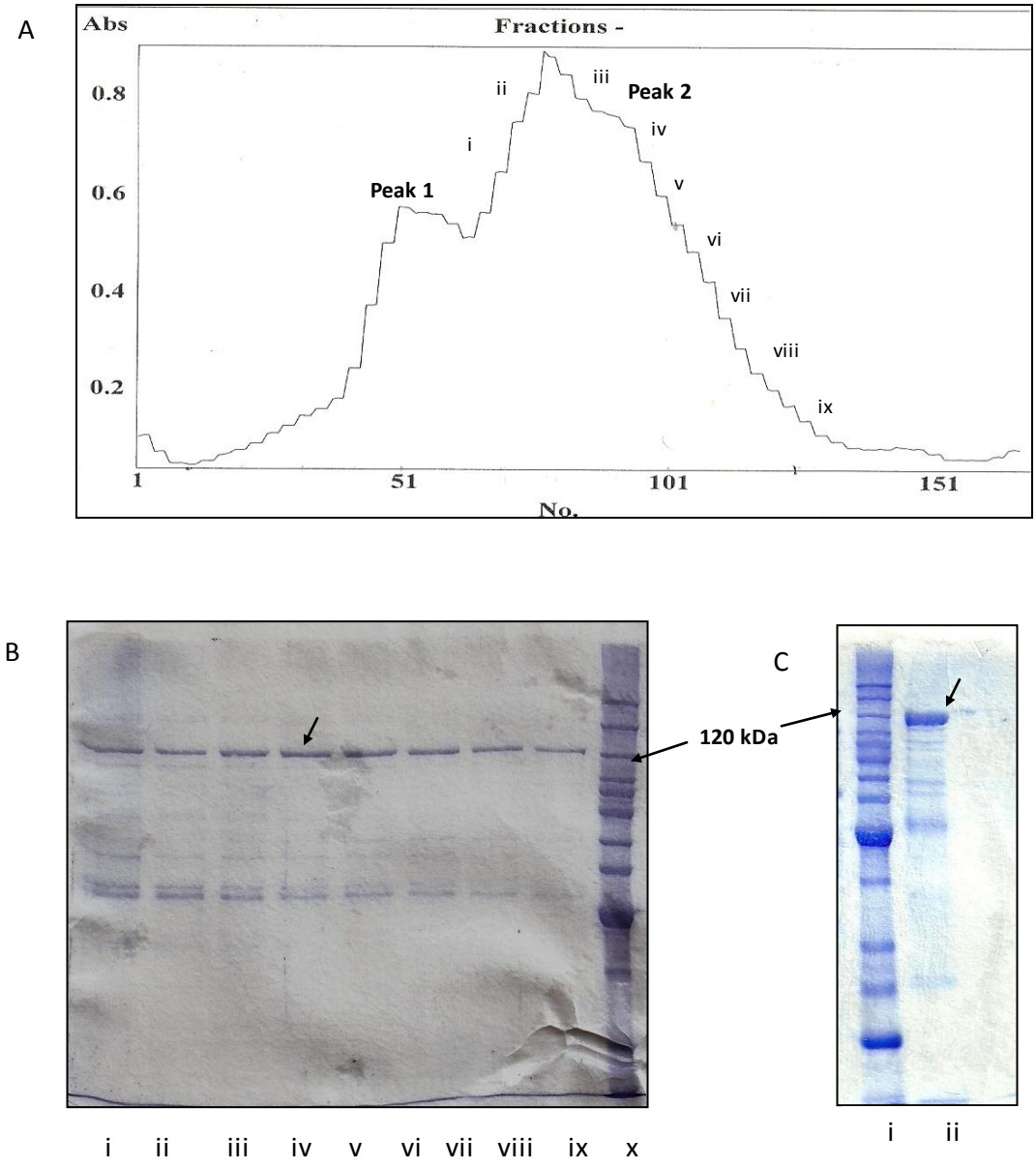

Figure 3-18: Ion-exchange chromatography using DEAE cellulose to isolate PEX6; (A) Elution profile of protein assayed at A_{280} nm when passed through DEAE column. (B) Lanes i - ix contain the protein fractions eluted from DEAE column and are separated by SDS-PAGE. The arrow in lane iv shows the position of the desired protein, PEX6. Lane x contains protein markers. (C) Lane ii contains the pooled and concentrated PEX6 (shown by arrow). Lane i contains protein markers.

4. DISCUSSION

4.1. Purification of a subset of *Saccharomyces cerevisiae* peroxisomal proteins

The work described in this thesis has been focused on the construction of plasmids encoding yeast peroxisomal proteins and the optimization of conditions for their expression and purification. Each protein presented a different set of challenges which made trouble shooting various procedures a major part of the work.

4.1.1. Purification of IDP3

The conditions for expression of IDP3 were determined easily and produced a good yield of intracellular protein. On purification, an unusual problem arose early in the purification scheme when it was found that the protein precipitated during the early streptomycin sulfate fractionation. The procedure was used successfully for other proteins to remove nucleic acids and associated proteins and even the inclusion of a number of different salts did not improve the situation. Ultimately, the crude extract was added directly to the nickel affinity column without the cleaning step, which in fact simplified the procedure.

Initially, the IMAC nickel column presented the problem that the IDP3 protein would not bind to it. A second resin, Ni-NTA was investigated and found to bind the protein very strongly leading to its ultimate purification. A possible explanation for this apparent inconsistency lies in the chelating matrix in the two resins. The IMAC resin employs iminodiacetic acid which has available only three chelating sites for each metal ion which binds the metal ions more weakly allowing ion leaching when in contact with strongly chelating proteins. This results in low affinity and metal-ion contamination in the eluted protein (Wahle et al., 1999). It allows the binding of different metal ions

including Cu, Ni, and Zn and has been used to purify a wide range of proteins (Sulkowski, 1985), but would not work for IDP3. The successful nitrilotriacetic acid resin has a fourth chelating site allowing ocupation of four ligand sites on the metal ion coordination sphere. Only two sites are free for interaction with the His tag, but this is sufficient for tight and efficient binding (Steinert et al., 1999). In the case of IDP3, the resin was successful in providing a one step > 95% purification.

4.1.2. Purification of PEX18 and PEX21

PEX18 and PEX21 presented the unusual problem of apparent low levels of expression during the initial trials. The reasons for this were not immediately obvious but one possibility lay in aberrant folding that resulted in the proteins being degraded by proteolysis even under conditions of rapid expression. A number of approaches were investigated to improve the protein yield. The first was to employ *E. coli* Rosetta BL21 cells in order to eliminate possible codon bias arising from the lack of tRNAs recognizing AGG and AGA codons. The Rosetta strain encodes tRNAs that recognize AGG, AGA, AUA, CUA, CCC and GGA on the pRARE plasmid (Rosenberg et al 1993), but ultimately it did not lead to an enhancement in expression levels. Subsequently, an *E. coli* Tuner strain in which a *lacY* mutation makes possible an IPTG concentration-dependent level of induction from very low to very high levels (Prinz et al, 1997) was investigated, but did not improve the yield of either protein.

In the end, successful expression of PEX18 and PEX21 was realized by transferring the His tag to the C-terminal end. This confirmed the earlier conjecture that the His-tag at the N-terminal end was interfering with the initial stages of protein folding.

With the His tag in the C-terminal location, the core of the protein appears to fold sufficiently well that the additional protein added late in translation does not interfere.

PEX18 presented the peculiar property of migrating as an apparently 42 kDa protein on SDS-PAGE whereas its actual size is 32 kDa. This is not entirely unusual among proteins with another example being the subunit of catalase HPII of *E. coli* which consistently migrates at 94 kDa despite its 84 kDa size. The most probably explanation lies in the amino acid composition that results in more SDS association with these proteins than is normal.

After finally being successfully expressed, PEX18 and PEX21 presented a second major problem with purification. Several different methods were investigated unsuccessfully. Particularly frustrating was the apparent low affinity of the proteins for nickel affinity resins. This problem was eventually circumvented by denaturing the proteins to expose more fully the His tag. This necessitated the inclusion of a subsequent renaturation step which could have been problematic, but proved to present no problems. Both proteins refolded into a stable and soluble structure during dialysis to remove the denaturant.

4.1.3. Purification of PEX6

Attempts to express and purify PEX6 presented a number of problems that were never fully solved. The levels of expression remained very low despite resorting to the Rosetta and Tuner strains and to media with metabolites such as glycerol that might have enhanced expression or encouraged protein folding. Because of time constraints, the solution for PEX18 and PEX21, transferring the His tag to the C-terminal end was not attempted and this may yet prove to be a solution for future work. The low yields of

protein may be part of the reason for the poor success in subsequent purification attempts. Surprisingly, ion exchange proved to be the most promising, but protein in sufficient quantity and of sufficient purity to proceed to crystallization trials was never obtained. Here again resorting to a His tag on the C-terminal end of the protein may allow the protein to be purified by nickel affinity chromatography. On the other hand, PEX6 is a very large protein at 112 kDa and it may be the shear size of the protein that is limiting expression and purification.

4.2. Future directions

The obvious direction for this project that should take place immediately is to take the three purified proteins on to crystallization trials and ultimately to solve their crystal structures. Once the crystal structures are known and mechanistic insights realized, a site directed mutagenesis study of the proteins can be undertaken with a focus on the catalytic centers or protein binding domains of the proteins. This may lead ultimately to a better understanding of some of the peroxisomal-based diseases that involve one or more of the target proteins.

5. REFERENCES

Agne, B., (2003) Pex8p: an intraperoxisomal organizer of the peroxisomal import machinery. *Mol. Cell* **11,** 635-646.

Alberts, B., Johnson, A., Lewis, J., Raff, M., Roberts, K., and Walter, P., (2002) Chapter 12: Peroxisomes. *Mol. Biol. Cell* (Fourth Edition), New York, Garland Science.

Brown, L., and Baker, A., (2008) Shuttles and cycles: transport of proteins into the peroxisome matrix. *Mol. Memb. Biol.* **25,** 363-375.

Braverman, N., Steel, G., Obie, C., Moser, A., Moser, H., Gould, S. J. and Valle, D. (1997) Human PEX7 encodes the peroxisomal PTS2 receptor and is responsible for Rhizomelic Chondrodysplasia punctata. *Nat. Genet*. **15**, 369-376.

Birschmann, I., Rosenkranz, K., Erdmann, R., and Kunau, W. H. (2005) Structural and functional analysis of the interaction of the AAA-peroxins Pex1p and Pex6p. *FEBS J.* **272**, 47–58.

Braverman, N. (1995) Disorders of peroxisomal biogenesis. *Human Mol. Gen.* **4**, 1791-1798.

De Duve, C., and Baudhuin, P. (1966) Peroxisomes (microbodies and related particles). *Physiol. Rev*. **46**, 323-357.

del Rio, L. A., Sandalio, L. M., Palma, J. M., Buena, P., and Corpas, F. J. (1992) Metabolism of oxygen radicals in peroxisomes and cellular implications. *Free Radical Biol. Med*. **13**, 557-80.

Dodt, G., and Gould, S. J. (1996) Multiple PEX genes are required for proper subcellular distribution and stability of Pex5p, the PTS1 receptor: evidence that PTS1 protein import is mediated by a cycling receptor. *J. Cell Biol.* **135,** 1763-1774.

Elgersma, Y. (1997) Overexpression of Pex15p, a phosphorylated peroxisomal integral membrane protein required for peroxisome assembly in S.cerevisiae, causes proliferation of the endoplasmic reticulum membrane. *EMBO J*. **16,** 7326-41.

Elgersma, Y., Vos, A., van den Berg, M., van Roermund, C. W., van der Sluijs, P., Distel, B., and Tabak, H. F. (1996) Peroxisomal beta-oxidation of polyunsaturated fatty acids in Saccharomyces cerevisiae: isocitrate dehydrogenase provides NADPH for reduction of double bonds at even positions. *J. Biol. Chem*. **271,** 26375–26382.

Erdmann, R., and Kunau, W.H. (1994) Purification and immunolocalization of the peroxisomal 3-oxoacyl-CoA thiolase from *Saccharomyces cerevisiae*. *Yeast* **10,** 1173–1182.

Erdmann, R. (1991) *PAS1*, a yeast gene required for peroxisome biogenesis, encodes a member of a novel family of putative ATPases. *Cell* **64,** 499–510.

Einwachter, H., Sowinski, S., Kunau, W. H., and Schliebs, W. (2001) *Yarrowia lipolytica* Pex20p, *Saccharomyces cerevisiae* Pex18p/Pex21p and mammalian Pex5pL fulfil a common function in the early steps of the peroxisomal PTS2 import pathway. *EMBO Rep*. **2,** 1035–1039.

Erdmann, R., and Schliebs, W. (2005) Peroxisomal matrix protein import: the transient pore model. *Nat*. *Rev*. *Mol. Cell Biol.* **6,** 738-42.

Ewald, H., and Motley, M. (2009) How peroxisomes multiply? *J. Cell Sc.* **122**, 2331-2336.

Faber, K. N., Heyman, J. A., and Subramani, S. (1998) Two AAA family peroxins, PpPex1p and PpPex6p, interact with each other in an ATP-dependent manner and are associated with different subcellular membranous structures distinct from peroxisomes. *Mol. Cell. Biol.* **18**, 936–943.

Gabaldon, T. (2010) Peroxisome diversity and evolution. *Philos. Trans. R. Soc. Lond. B. Biol. Sci.* **365**, 765-773.

Gould, S. J., Keller, G. A., and Subramani, S. (1987) Identification of peroxisomal targeting signals located at the carboxy terminus of four peroxisomal proteins. *J. Cell Biol.* **105,** 2923–2931.

Gould, S. J., Raymond, T., and Valle, M. (2001) The Peroxisome Biogenesis Disorders. *The Metabolic and Molecular Basis of Inherited Disease.* 3181-3218.

Güldener, U., Heck, S., Fiedler, T., Beinhauer, J. and Hegemann, J. H. (1996) A new efficient gene disruption cassette for repeated use in budding yeast. *Nucleic Acids Res.* **24,** 2519–2524.

Haselbeck, R. J., and McAlister, H. L. (1993) *J. Biol. Chem*. **268,** 12116–12122.

Hashiguchi, N., Kojidani, T., Imanaka, T., Haraguchi, T., Hiraoka, Y., Baumgart, E., Yokota, S., Tsukamoto, T., and Osumi, T. (2002) Peroxisomes are formed from complex membrane structures in PEX6-deficient CHO cells upon genetic complementation. *Mol. Biol. Cell* **13**, 711–722.

Haselbeck, R. J., Loftus, T., and McAlister, H. L. (1991) Kinetic Properties and Metabolic Contributions of Yeast Mitochondrial and Cytosolic NADP+-specific Isocitrate Dehydrogenases. *J. Biol. Chem*. **266,** 2339–2345.

Henke, B., Wolfgang, G., Veronique, B., and Ralf, E. (1998) *IDP3* Encodes a Peroxisomal NADP-dependent Isocitrate Dehydrogenase required for the -Oxidation of Unsaturated Fatty Acids. *J. Biol. Chem*. **273**, 3702–3711.

Hettema, E. H., Distel, B., and Tabak, H. F. (1999) Import of proteins into peroxisomes. *Biochim. Biophys. Acta* **1451**, 17-34.

Hettema, E.H., and Motley A.M. (2009) How peroxisomes multiply? *J. Cell Sci.* **122**, 2331-2336.

Hashimoto, T. (1982) Biosynthesis of enzymes of rat-liver mitochondrial β-oxidation *Ann. N. Y. Acad. Sci.* **386,** 5–12.

Kunau, W. H., Dommes, V., and Schulz, H. (1995) Beta-oxidation of fatty acids in mitochondria, peroxisomes, and bacteria: a century of continued progress. *Prog. Lipid Res.* **34**, 267-342.

Kiel, J.A., Hilbrands, R. E., van der Klei, I. J., Rasmussen, S. W., Salomons, F. A., van der Heide, M., Faber, K. N., Cregg, J. M., and Veenhuis, M. (1999) Hansenula polymorpha Pex1p and Pex6p are peroxisome-associated AAA proteins that functionally and physically interact. *Yeast* **15**, 1059–1078.

Krzywda, S., Brzozowski, A. M., Verma, C., Karata, K., Ogura, T., Wilkinson, A. J. (2002) The crystal structure of the AAA domain of the ATP-dependent protease FtSH of *Escherichia coli* at 1.5 Å resolution**.** *Structure* **10**, 1073-1083.

Kunau, W. H., Buhne, S., de la Garza, M., Kionka, C., Mateblowski, M., and Schulz, H. (1995) Beta-oxidation of fatty acids in mitochondria, peroxisomes, and bacteria: a century of continued progress. *Prog. Lipid Res.* **34**, 267–342.

Lazarow, P. B. (2003) Peroxisome biogenesis: advances and conundrums. *Curr. Op. Cell Biol.* **15**, 489-497.

Lazarow, P. B., and Fujiki, Y. (1985) Biogenesis of peroxisomes. *Annu. Rev. Cell Biol.* **1**, 489-530.

Lanyon-Hogg, T., Warriner, S. L., and Baker, A. (2010) Getting a camel through the eye of a needle: the import of folded proteins by peroxisomes. *Biol. Cell.* **102,** 245-63.

Leon, S., Goodman, J. M., and Subramani, S. (2006) Uniqueness of the mechanism of protein import into the peroxisome matrix: transport of folded, co-factor-bound and oligomeric proteins by shuttling receptors. *Biochim. Biophys. Acta.* **1763,** 1552-64.

Mozdy, A. D. (2000) Dnm1p GTPase-mediated mitochondrial fission is a multi-step process requiring the novel integral membrane component Fis1p. *J Cell Biol* **151**, 367-380.

Matsumoto, N., Tamura, S., and Fujiki, Y. (2003) The pathogenic peroxin Pex26p recruits the Pex1p-Pex6p AAA ATPase complexes to peroxisomes. *Nat. Cell Biol.* **5**, 454-460.

McAlister, H., Hall, L. M., and Anderson, S. L. (1994) *Biochemistry* **33,** 9661–9667.

Mannaerts, A., and van Veldhoven, A. (1990) The peroxisome: functional properties in health and disease. *Biochemical Society (Great Britain) Transcripts* **18**, 87-89.

Ogura, T., and Wilkinson, A. J. (2001) AAA+ superfamily ATPases: common structure – diverse function. *Genes* **6**, 575–597.

Purdue, P. E., and Lazarow, P. B. (2001) Peroxisome biogenesis. *Annu. Rev. Cell Dev. Biol.* **17**, 701-752.

Purdue, P. E., Yang, X., and Lazarow, P.B. (1998) Pex18p and Pex21p, a novel pair of related peroxins essential for peroxisomal targeting by the PTS2 pathway *J. Cell Biol* **143,** 1859–1869.

Purdue P. E., and Lazarow P. B. (2001) 'Pex18p Is Constitutively Degraded during Peroxisome Biogenesis' *The Journal of Biological Chemistry* **276**, 47684–47689.

Platta, H. W. (2005) Functional role of the AAA peroxins in dislocation of the cycling PTS1 receptor back to the cytosol. *Nat. Cell Biol* **7**, 817-22.

Paul, A. M. M., Juliette M., Hanane K., Nathalie G., Murielle H., and Veronique, H. (2005) Peroxisomes, glyoxysomes and glycosomes (Review), *Mol. Mem. Biol.* **22**, 133-145.

Qian, L., McAlister, H. (2010) Peroxisomal localization and function of $NADP^+$-specific Isocitrate dehydrogenases in yeast, *Arch. Biochem and Biophys.* **493**, 125–134.

Rhodin, J. (1954) Correlation of ultra structural organization and function in normal and experimentally changed proximal convoluted tubule cells of the mouse kidney. Ph.D. thesis. Karolinska Institutet, Aktiebolaget Godvil, Stockholm.

Rooij, I. (2010) A role for the dynamin-like protein Vps1 during endocytosis in yeast. *J. Cell Sci.* **123,** 3496-506.

Ralf, E., and Wolfgang, S. (2005) Cycling peroxisome import receptors, *Nat. Rev. Mol. Cell Biol.* **6**, 738-742.

Schrader, M., and Fahimi, H. D. (2006) Growth and division of peroxisomes. *Int. Rev. Cytol.* **255**, 237-290

Stephen, J. G. and Cynthia, S. C. (2002) Peroxisomal-protein import: is it really that complex? *Nat. Rev. Mol. Cell Biol.* **3**, 382-389

Subramani, S. (2002) Import of proteins into peroxisomes. *Prot. Targeting Trans. Transloc* **2,** 268-292.

Schulz-Borchard, U., and Thieringer, R. (1988) *Biochem. Soc. Trans.* **16,** 418–420.

Stein, K., Annette, S., Ralf, E., and Hanspeter, R. (2002) Interactions of Pex7p and Pex18p/Pex21p with the Peroxisomal Docking Machinery: Implications for the First Steps in PTS2 Protein Import. *Mol. Cell. Biol.* **88**, 6056–6069.

Schutgens, E. (1986) Peroxisomal disorders: A newly recognized group of genetic diseases. *Euro. J. Pedi* **144**, 430-440

Singh, R. (1997) Biochemistry of peroxisomes in health and disease. *Mol. Cell. Biochem.* **167**, 1-29.

Singh, T., Makoto H., Shoji, M., Yuko, A., Shino, G., and Mikio, N. (2009) Molecular components required for the targeting of PEX7 to peroxisomes in *Arabidopsis thaliana*, *The Plant J.* **60**, 488–498.

Tolbert, N. E. (1981) Metabolic Pathways in Peroxisomes and Glyoxysomes**.** *Annu. Rev. Biochem.* **50,** 133–157

Tabak, H. F., Hoepfner, D., Zand, A., Geuze, H. J., Braakman, I. and Huynen, M. A. (2006) Formation of peroxisomes: present and past. *Biochim. Biophys. Acta* **1763**, 1647-1654.

van den Bosch, H., Schutgens, R. B.H., Wanders, R. J.A., and Tager, J.M. (1992) Biochemistry of Peroxisomes. *Annu. Rev. Biochem.* **61,** 157–197.

Veenhuis, M., Mateblowski, M., Kunau, W.H., and Harder, W. (1987) Proliferation of microbodies in *Saccharomyces cerevisiae***.** *Yeast* **3**, 77–84.

van Roermund, C. W. T., Elgersma, Y., Singh, N., Wanders, J. A., and Tabak, H. F. (1995) The membrane of peroxisomes in Saccharomyces cerevisiae is impermeable to NAD (H) and acetyl-CoA under *in vivo* conditions. *EMBO J.* **14**, 3480–3486.

Vladimir, I. Titorenko, H., Richard, A., and Rachubinski, T. (2001) The life cycle of the peroxisome. *Nat. Rev. Mol. Cell Biol.* **2**, 357-368.

Wanders, R. J. (1995) Peroxisomal disorders: a review, *J. Neuropath. Exp. Neurol.* **54**, 726-739.

Wolf, J., Schliebs, W., and Erdmann, R. (2010) Peroxisomes as dynamic organelles: peroxisomal matrix protein import. *FEBS J.* **277**(16):3268-78.

Wanders, R. J. and Waterham, H. R. (2006) Biochemistry of mammalian peroxisomes revisited. *Annu. Rev. Biochem.* **75**, 295-332.

Zhang, X., Shaw, A., Bates, P. A., Newman, R. H., Gowen, B., Orlova, E., Gorman, M. A., Kondo, H, Dokurno, P., Lally, J., Leonard, G., Meyer, H., van Heel, T., and Freemont, M. (2000) Structure of the AAA ATPase p97. *Mol. Cell* **6,** 1473-1476.